


ORIGINAL ARTICLE

WILEY **MOLECULAR ECOLOGY**

Idiosyncratic responses to climate-driven forest fragmentation and marine incursions in reed frogs from Central Africa and the Gulf of Guinea Islands

Rayna C. Bell^{1,2,3}  | Juan L. Parra⁴ | Gabriel Badjedjea⁵ | Michael F. Barej⁶ | David C. Blackburn^{7,8} | Marius Burger^{9,10} | Alan Channing¹¹ | Jonas Maximilian Dehling¹² | Eli Greenbaum¹³ | Václav Gvoždík^{14,15} | Jos Kielgast^{16,17} | Chifundera Kusamba¹⁸ | Stefan Lötters¹⁹ | Patrick J. McLaughlin²⁰ | Zoltán T. Nagy^{6,21} | Mark-Oliver Rödel⁶ | Daniel M. Portik^{2,22} | Bryan L. Stuart²³ | Jeremy VanDerWal^{24,25} | Ange Ghislain Zassi-Boulou²⁶ | Kelly R. Zamudio³

¹Department of Vertebrate Zoology, National Museum of Natural History, Smithsonian Institution, Washington, DC, USA

²Museum of Vertebrate Zoology, University of California, Berkeley, CA, USA

³Department of Ecology and Evolutionary Biology, Cornell University, Ithaca, NY, USA

⁴Grupo de Ecología y Evolución de Vertebrados, Instituto de Biología, Universidad de Antioquia, Medellín, Colombia

⁵Département d'Ecologie et Biodiversité des ressources Aquatiques, Centre de Surveillance de la Biodiversité, Kisangani, Democratic Republic of the Congo

⁶Museum für Naturkunde - Leibniz Institute for Evolution and Biodiversity Science, Berlin, Germany

⁷Florida Museum of Natural History, University of Florida, Gainesville, FL, USA

⁸Department of Herpetology, California Academy of Sciences, San Francisco, CA, USA

⁹African Amphibian Conservation Research Group, Unit for Environmental Sciences and Management, North-West University, Potchefstroom, South Africa

¹⁰Flora Fauna & Man, Ecological Services Ltd., Tortola, British Virgin Islands

¹¹Biodiversity and Conservation Biology Department, University of the Western Cape, Bellville, South Africa

¹²Abteilung Biologie, Institut für Integrierte Naturwissenschaften, Universität Koblenz-Landau, Koblenz, Germany

¹³Department of Biological Sciences, University of Texas at El Paso, El Paso, TX, USA

¹⁴Institute of Vertebrate Biology, Czech Academy of Sciences, Brno, Czech Republic

¹⁵Department of Zoology, National Museum, Prague, Czech Republic

¹⁶Section of Freshwater Biology, Department of Biology, University of Copenhagen, Copenhagen, Denmark

¹⁷Center for Macroecology, Evolution and Climate, Natural History Museum of Denmark, Copenhagen, Denmark

¹⁸Laboratoire d'Herpétologie, Département de Biologie, Centre de Recherche en Sciences Naturelles, Lwiro, Democratic Republic of the Congo

¹⁹Biogeography Department, Trier University, Trier, Germany

²⁰Department of Biology, Drexel University, Philadelphia, PA, USA

²¹Royal Belgian Institute of Natural Sciences, Brussels, Belgium

²²Department of Biology, University of Texas, Arlington, TX, USA

²³North Carolina Museum of Natural Sciences, Raleigh, NC, USA

²⁴Centre for Tropical Biodiversity & Climate Change, College of Science and Engineering, James Cook University, Townsville, Qld, Australia

²⁵Division of Research and Innovation, eResearch Centre, James Cook University, Townsville, Qld, Australia

²⁶Institut National de Recherche en Sciences Exactes et Naturelles, Brazzaville, République du Congo

Correspondence

Rayna C. Bell, Department of Vertebrate Zoology, National Museum of Natural History, Smithsonian Institution, Washington, DC, USA.
Email: bellrc@si.edu

Funding information

Explorer's Club; American Philosophical Society; Sigma Xi; Society of Systematic Biologists; Mario Einaudi Center for International Studies; Cornell Graduate School; Andrew W. Mellon Foundation; EEB Paul P. Feeny Fund; EEB Paul Graduate Fellowship; University of California President's Postdoctoral Fellowship; Museum of Comparative Zoology Herpetology Division at Harvard University; BIOTA projects of the Federal Ministry of Education and Research; BIOTA Germany Grant numbers 01 LC 0017 and 01 LC 0025; US National Science Foundation, Grant/Award Number: DEB-1309171, DEB-1202609, DEB-1145459; National Geographic Society, Grant/Award Number: 8556-08, 8868-10; California Academy of Sciences; Percy Sladen Memorial Fund; IUCN/SSC Amphibian Specialist Group; Department of Biology at Villanova University; University of Texas at El Paso; Czech Science Foundation, Grant/Award Number: 15-13415Y; Ministry of Culture of the Czech Republic, Grant/Award Number: DKRVO 2017/15; National Museum, Grant/Award Number: 00023272

Abstract

Organismal traits interact with environmental variation to mediate how species respond to shared landscapes. Thus, differences in traits related to dispersal ability or physiological tolerance may result in phylogeographic discordance among co-distributed taxa, even when they are responding to common barriers. We quantified climatic suitability and stability, and phylogeographic divergence within three reed frog species complexes across the Guineo-Congolian forests and Gulf of Guinea archipelago of Central Africa to investigate how they responded to a shared climatic and geological history. Our species-specific estimates of climatic suitability through time are consistent with temporal and spatial heterogeneity in diversification among the species complexes, indicating that differences in ecological breadth may partly explain these idiosyncratic patterns. Likewise, we demonstrated that fluctuating sea levels periodically exposed a land bridge connecting Bioko Island with the mainland Guineo-Congolian forest and that habitats across the exposed land bridge likely enabled dispersal in some species, but not in others. We did not find evidence that rivers are biogeographic barriers across any of the species complexes. Despite marked differences in the geographic extent of stable climates and temporal estimates of divergence among the species complexes, we recovered a shared pattern of intermittent climatic suitability with recent population connectivity and demographic expansion across the Congo Basin. This pattern supports the hypothesis that genetic exchange across the Congo Basin during humid periods, followed by vicariance during arid periods, has shaped regional diversity. Finally, we identified many distinct lineages among our focal taxa, some of which may reflect incipient or unrecognized species.

KEYWORDS

climatic refugia, ecological niche modelling, *Hyperolius*, land-bridge island, lineage divergence, riverine barriers

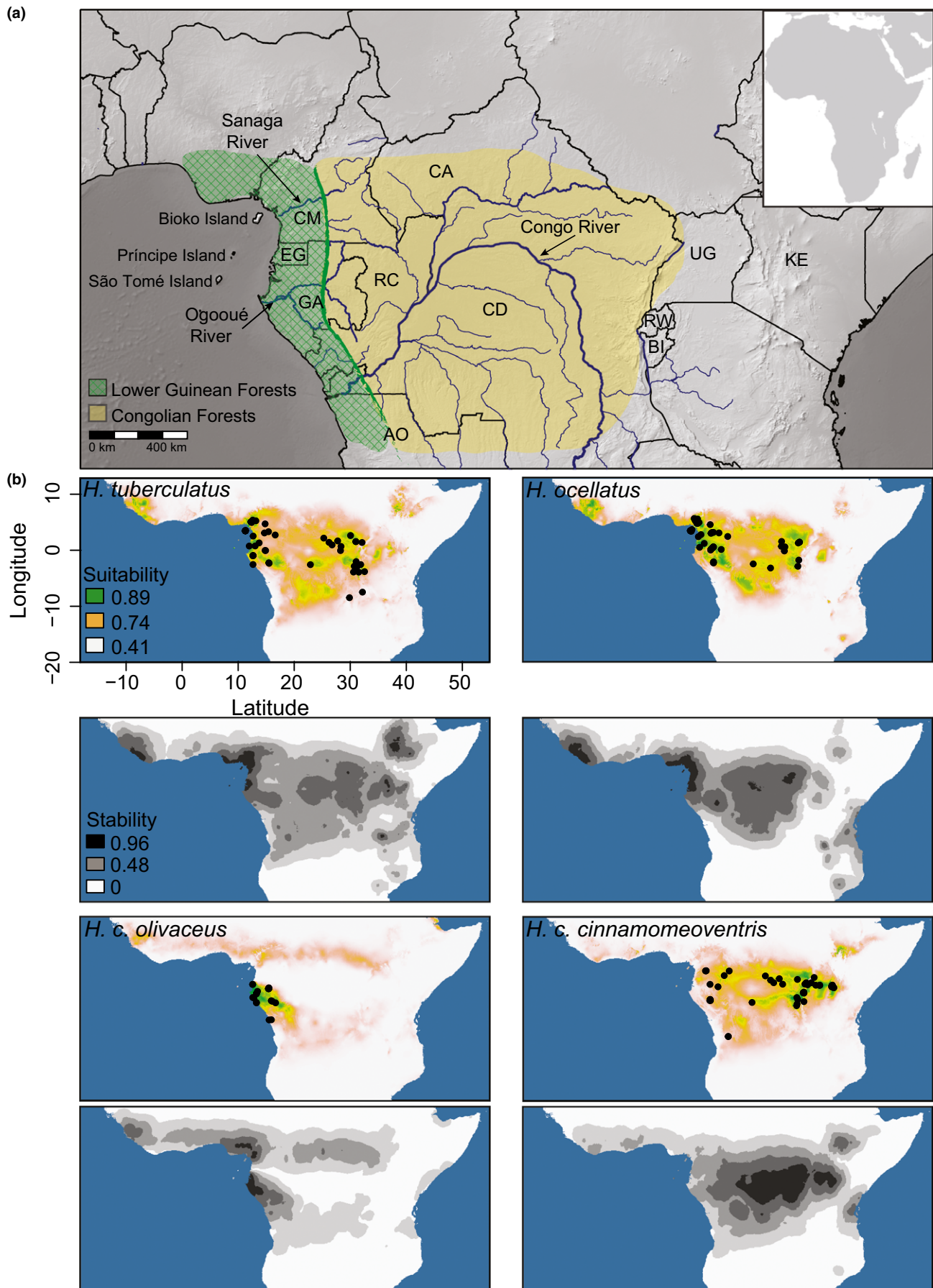
1 | INTRODUCTION

Trait variation among and within species impacts how populations respond to environmental variation, which can result in both temporal and spatial discrepancy in the distribution of phylogeographic structure among co-distributed species (Massatti & Knowles, 2014; Papadopoulou & Knowles, 2015; Paz, Ibáñez, Lips, & Crawford, 2015). For example, body size and physiological breadth are directly related to dispersal ability and the capacity to colonize new environments; thus, these traits likely influence the frequency of migration and gene flow among subdivided populations (Papadopoulou & Knowles, 2015; Rodríguez et al., 2015). Likewise, traits related to

species recognition and mate choice may indirectly affect the distribution of genetic diversity via sexual selection, assortative mating and inbreeding avoidance (reviewed in Zamudio, Bell, & Mason, 2016). Consequently, interactions between species-specific traits and environmental variation may result in phylogeographic discordance among co-distributed taxa, even when they are responding to common landscape barriers (Papadopoulou & Knowles, 2016). Here we investigate how co-distributed, colour polymorphic reed frog species (Hyperoliidae: *Hyperolius*) that vary in ecological breadth have responded to a shared climatic history across Central Africa.

The Lower Guineo-Congolian forests extend across the Congo Basin from the Albertine Rift in East Africa westward to the Atlantic

FIGURE 1 (a) Major biogeographic features of the Lower Guinean and Congolian forests of Central Africa. Country abbreviations: AO (Angola), BI (Burundi), CA (Central African Republic), CD (Democratic Republic of the Congo), CM (Cameroon), EG (Equatorial Guinea), GA (Gabon), KE (Kenya), RC (Republic of Congo), RW (Rwanda), UG (Uganda). (b) Full-parameter modelled distribution of current suitable climate and dynamic stability estimated over the last 120 ky for the *Hyperolius tuberculatus* complex, *H. ocellatus* complex, *H. c. olivaceus* and *H. c. cinnamomeoventris*



Ocean (Figure 1; Linder et al., 2012) and host much of the world's biodiversity (Jenkins, Pimm, & Joppa, 2013; Lewin et al., 2016). A number of studies support periods of climate-driven diversification (Bohoussou et al., 2015; Born et al., 2011; Dauby, Duminil, et al., 2014; Duminil et al., 2015; Hassanin et al., 2015; Jacquet et al., 2015; Johnston & Anthony, 2012; Leaché & Fujita, 2010; Nicolas et al., 2011; Plana, 2004; Quéroutil, Verheyen, Dillen, & Colyn, 2003; Tosi, 2008) and cycles of vicariance and genetic exchange across the northern Congo Basin (Bowie, Fjeldsø, Hackett, & Crowe, 2004; Couvreur, Chatrou, Sosef, & Richardson, 2008; Fjeldsø & Lovett, 1997; Kadu et al., 2011; Tosi, 2008) as key mechanisms shaping the distribution of diversity in this region. Patterns of fine-scale phylogeographic structure in rainforest taxa (Born et al., 2011; Hardy et al., 2013; Koffi, Hardy, Doumenge, Cruaud, & Heuertz, 2011; Maley, 1996; Nicolas et al., 2011; Tosi, 2008) are consistent with persistence in a central refuge in the west-central Congo Basin and multiple smaller refugia throughout montane Cameroon and Gabon in western Central Africa (Maley, 1996); however, comparisons of molecular divergence among sister species reveal a continuum of divergence times ranging from Late Miocene (Duminil et al., 2013; Holstein & Renner, 2011; Njabo, Bowie, & Sorenson, 2008; Zimkus & Gvoždík, 2013; Zimkus et al., 2017) to Pleistocene (Bohoussou et al., 2015; Duminil et al., 2015; Jacquet et al., 2015; Johnston & Anthony, 2012; Nicolas et al., 2011; Tosi, 2008). Likewise, rivers are barriers to dispersal in many mammal and understory bird species across the Guineo-Congolian forest (Anthony et al., 2007; Bohoussou et al., 2015; Harcourt & Wood, 2012; Hassanin et al., 2015; Huntley & Voelker, 2016; Jacquet et al., 2015; Mitchell, Locatelli, Sesink Clee, Thomassen, & Gonder, 2015; Nicolas et al., 2011; Quéroutil et al., 2003; Telfer et al., 2003; Voelker et al., 2013), but appear to be less important for plants, reptiles and amphibians (Freedman, Thomassen, Buermann, & Smith, 2010; Kindler et al., 2016; Lowe, Harris, Dormontt, & Dawson, 2010; Zimkus et al., 2017). These idiosyncratic patterns suggest that differences in organismal traits (Heuertz, Duminil, Dauby, Savolainen, & Hardy, 2014; Kindler et al., 2016; Ley et al., 2014), mediated by ecotones on small spatial scales (Freedman et al., 2010; Jacquet et al., 2015; Smith, Wayne, Girman, & Bruford, 1997; Smith et al., 2011) and environmental gradients on large spatial scales (Dauby, Hardy, Leal, Breteler, & Stévant, 2014; Duminil et al., 2013; Kirschel et al., 2011; Smith et al., 2005), may explain why co-distributed species responded differently to a common landscape.

The Lower Guinean forests extend from continental Africa along the Gulf of Guinea archipelago. This chain of islands is comprised of a land-bridge island (Bioko) currently separated from mainland Africa by approximately 30 km of shallow sea, and three oceanic islands (Príncipe, São Tomé and Annobón) that have never been connected to continental Africa. The volcanic peaks that comprise Bioko Island formed 1–3 Mya (Deruelle et al., 1991; Marzoli et al., 2000) and since then, cycles of rising and retreating sea levels resulted in several periods of isolation and connectivity between Bioko and the adjacent continent (Meyers, Rosendahl, Harrison, & Ding, 1998). Relative to its size and age, Bioko Island

hosts high species diversity and most of this diversity is also found in mainland Guineo-Congolian forests (Jones, 1994). By contrast, the three oceanic islands are older (5–30 Myr), host lower overall species diversity, and most of this diversity is endemic (Jones, 1994). This pattern indicates that the exposed land bridge likely enabled a sizeable proportion of Guineo-Congolian biodiversity to colonize Bioko in a relatively short period of time whereas the oceanic islands slowly accumulated endemic diversity via sweepstakes overseas dispersal followed by in situ diversification. The diversity of *Hyperolius* reed frogs in the Gulf of Guinea archipelago mirrors this overall biogeographic pattern: the four species that occur on the land-bridge island are shared with the adjacent continental forests, whereas the three species that occur on the oceanic islands are single-island endemics. The most recent periods of high connectivity between Bioko and continental Guineo-Congolian forests coincided with the last glacial maximum (LGM; ~21 kya) and glacial period preceding the Last Interglacial (LIG; ~120 kya). Yet, a range of molecular divergence (Barej et al., 2014; Butynski & Koster, 1994; Leaché & Fujita, 2010; Melo, Warren, & Jones, 2011; Pérez, Fa, Castroviejo, & Purroy, 1994) indicates that for some taxa, populations on Bioko remained genetically isolated throughout this recent cycle of geographic connectivity, whereas in others, gene flow during periods of geographic connectivity may have obscured population divergence (Futuyama, 2010).

Here, we focus on three largely sympatric species complexes of *Hyperolius* reed frogs that inhabit rainforest, bushland (disturbed forest), and humid savannah habitats across the Lower Guineo-Congolian forests. We quantify environmental niche, climatic stability and phylogeographic divergence within each species complex to test whether differences in ecological breadth—environmental and physiological tolerance (Bonier, Martin, & Wingfield, 2007; López-Urbe, Zamudio, Cardoso, & Danforth, 2014)—correspond with temporal and spatial heterogeneity in species' responses to historical climatic fluctuations. Specifically, for the forest-dependent species complexes (*H. ocellatus* and *H. tuberculatus*), we expect estimates of environmental niche will reflect narrow ecological breadth and thus a history of fragmented climatic stability with centres of endemism concentrated in areas of high climatic stability. In the *Hyperolius cinnamomeoventris* complex, known from both forest and humid savannah habitats, we expect estimates of environmental niche will reflect wide ecological breadth and consequently more contiguous habitat stability and population connectivity through time. Two of our focal species complexes (*H. ocellatus* and *H. tuberculatus*) also occur on Bioko Island, whereas the third (*H. cinnamomeoventris*) is absent. We further predict that differences in the distribution of suitable habitat across the land bridge may also explain why some reed frog species have colonized the island and others have not. Finally, we assess how genetic diversity, proposed biogeographic barriers (climatic refugia and rivers) and regional phenotypic variation (sexual dichromatism and colour polymorphism) correspond to our current understanding of taxonomic diversity within each species complex.

2 | MATERIAL AND METHODS

2.1 | Focal species and sampling details

We identified each of the focal reed frog species complexes for this study by selecting the smallest unit of monophyletic lineages whose combined ranges encompass the Lower Guineo-Congolian forests. Species of the *Hyperolius cinnamomeoventris* complex are the few reed frogs that inhabit both bushland (disturbed forest) and humid savannah habitats (Schlötter, 1999). The vast majority of the *H. cinnamomeoventris* species complex range is attributed to the subspecies *H. c. cinnamomeoventris*, and the rest of the complex is comprised of *H. veithi* from the Congo Basin (Schick et al., 2010), the subspecies *H. c. olivaceus* in Gabon (Laurent, 1943; Schick et al., 2010) and three species (*H. thomensis*, *H. malleri* and *H. drewesi*) endemic to the oceanic islands of São Tomé and Príncipe (Figure 2a; Bell, Drewes, & Zamudio, 2015; Bell, 2016). Coloration across most of the species complex range is sexually dichromatic (males and females differ in coloration); however, *H. veithi* and the island endemics are sexually monochromatic (Figure 2d). For this study, we collected 129 samples from 61 localities (Table S1) including type localities of *H. cinnamomeoventris* (Duque de Bragança, Angola), *H. veithi* (Salonga National Park, Democratic Republic of the Congo), *H. malleri* and *H. thomensis* (São Tomé Island), *H. drewesi* (Príncipe Island) and *H. c. olivaceus* (Lambaréné, Gabon; Figure 2a).

Species of the *H. tuberculatus* complex occur in bushland and rainforest edge habitats where they can be found far from reproductive sites; consequently, frogs in this species complex are hypothesized to have high dispersal abilities and tolerance for habitat disturbance (Amiet, 2012). Coloration, pattern and sexual dichromatism vary widely across the range of the species complex (Figure 3d), which includes *H. tuberculatus* in west Central Africa, *H. hutsebauti* north of the Congo River in eastern Central Africa (Laurent, 1956, 1976; Schlötter, 1999), and *H. dintelmanni* in montane south-western Cameroon (Amiet, 2012; Lötters & Schmitz, 2004; Portik et al., 2016). We collected 104 samples from 47 localities (Table S1) including the type localities of *H. tuberculatus* (Lambaréné, Gabon) and *H. dintelmanni* (Bakossi Mountains, Cameroon), sites near the type locality of *H. hutsebauti* (Ibembo, Democratic Republic of the Congo), and Bioko Island (Figure 3a).

Finally, species of the *H. ocellatus* complex occur in evergreen, semi-deciduous and gallery forests and are sexually dichromatic throughout the range with regional variation in female coloration (Figure 4d); morphotypes 1 and 2 occur north of the Sanaga River in Cameroon (*H. o. ocellatus*), and morphotype 3 (*H. o. purpurescens*) occurs south of the Sanaga River and across the rest of the species complex range (Amiet, 2012; Laurent, 1943; Perret, 1975). We collected 137 samples from 39 localities (Table S1) including the three regional female colour morphs, the type locality of *H. ocellatus* (Bioko Island, Equatorial Guinea) and the type locality of *H. o. purpurescens* (Kisangani, Democratic Republic of the Congo; Figure 4a).

Tissue samples (toe clips, liver or muscle) were preserved in 95% ethanol or RNAlater and voucher specimens are deposited in the

Cornell University Museum of Vertebrates, the California Academy of Sciences, the North Carolina Museum of Natural Sciences, the U.S. National Museum of Natural History, the University of Texas at El Paso Biodiversity Collections, the Museum of Comparative Zoology at Harvard University, the Peabody Museum at Yale University, the Museum of Vertebrate Zoology at the University of California Berkeley, Museum für Naturkunde in Berlin, the National Museum in Prague, the Institut National de Recherche sur les Sciences Exactes et Naturelles and the Royal Belgian Institute of Natural Sciences in Brussels (Table S1). Samples without catalogue numbers are maintained in research collections of coauthors AC, MB, JK and SL.

2.2 | Ecological niche modelling

We compiled a database of vouchered occurrences from our own fieldwork and mappable museum specimen records in VERTNET (www.vertnet.org) that could confidently be attributed to each species complex based on locality, genetic and/or morphological examination. The final database included 65, 57 and 46 localities for the *H. cinnamomeoventris*, *H. tuberculatus* and *H. ocellatus* species complexes, respectively (Table S1). Due to deep genetic divergence within the *H. cinnamomeoventris* complex dating to the mid-Miocene (Bell, Drewes, Channing, et al., 2015; Schick et al., 2010) and potential for niche divergence over this time period, we ran separate models for *H. c. olivaceus* (20 unique localities) and *H. c. cinnamomeoventris* (45 unique localities). We excluded *H. veithi* and the island endemics from these analyses because the limited geographic distribution of these four species precludes sufficient sampling to generate individual models. The model for the *H. tuberculatus* complex included all three recognized species (*H. tuberculatus*, *H. dintelmanni* and *H. hutsebauti*) and that for the *H. ocellatus* complex included the two recognized subspecies (*H. o. ocellatus* and *H. o. purpurescens*).

We estimated the niche and potential geographic distribution of *H. c. cinnamomeoventris*, *H. c. olivaceus* and the *H. tuberculatus* and *H. ocellatus* complexes under current climatic conditions using presence records and a maximum entropy algorithm (MAXENT v. 3.3.3k; Phillips, Anderson, & Schapire, 2006). MAXENT, a robust method for inferring ENMs when only presence data are available, estimates the relationship between occurrences and environmental variables based on the environments sampled by occurrences relative to all available environments in the study area. Following Soberón (2007), we specified a study area for the ENMs that represents the potential area the focal species can access given their dispersal or colonization ability. The genus *Hyperolius* is distributed throughout sub-Saharan Africa; thus, our study area included continental Africa and the Gulf of Guinea islands, but we restricted the upper limit of the study area by the distribution of the Sahara Desert and the North Saharan steppe and woodlands (Olson & Dinerstein, 2001). Given that our focal taxa were not sampled randomly across the study area (sub-Saharan Africa), we applied the same sampling bias to the selection of background points for the model (Elith et al., 2011) using a sampling effort surface based on all mappable anuran specimen records

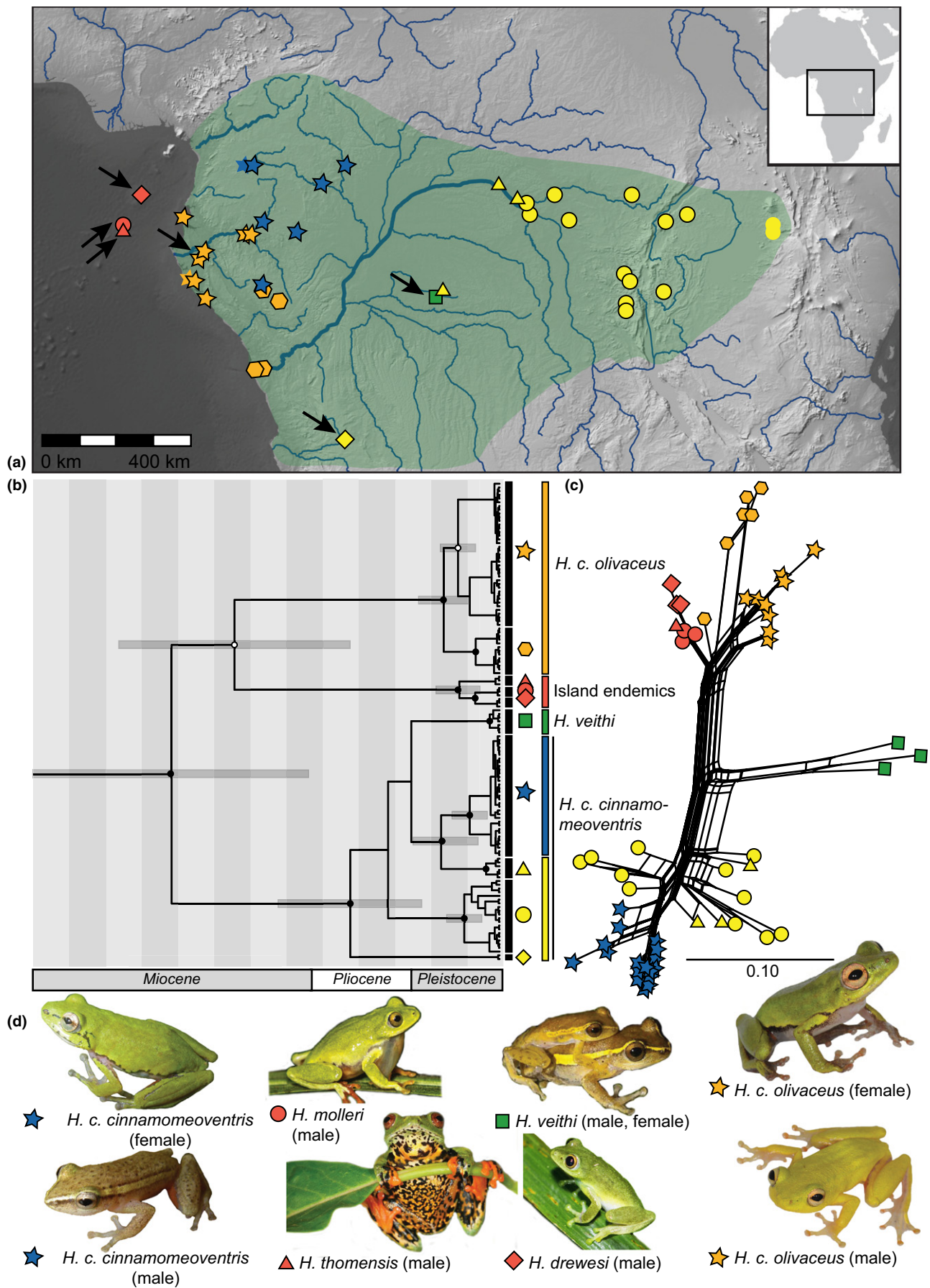


FIGURE 2 (a) Distribution of *Hyperolius cinnamomeoventris* species complex sampling localities in Central Africa including the islands of São Tomé and Príncipe. The approximate range is shown in green and the type localities for *H. c. cinnamomeoventris*, *H. veithi*, *H. thomensis*, *H. mollerii*, *H. drewesi* and *H. c. olivaceus* are indicated with black arrows. Symbols without black borders reflect localities with only mtDNA sequence data. (b) Mitochondrial (16S and cytochrome *b*) phylogeography; posterior probabilities >.95 are denoted by black dots, probabilities >.85 are denoted by white dots, and 95% highest posterior density intervals for divergence time estimates on well-supported nodes are indicated. The axis indicates geological epochs (Miocene, Pliocene and Pleistocene) and time before present in increments of 1 million years. (c) Multilocus nuDNA networks generated using POAD and SPLITSTREE. In all cases, samples are coded with shapes corresponding to mitochondrial lineages. The scale represents genetic distance equally weighted across loci. (d) Representative photographs of female and male coloration. Photograph credits: A. Stanbridge, D. Lin, B. Stuart, J. Kielgast

from sub-Saharan Africa in VERTNET. We used the number of unique years that any anuran was collected at a site (resolution of 0.0083 degrees or ~1 km at the Equator) as an indicator of sampling effort. We aggregated this raster at a factor of 10 to produce a 10 × 10 km block, summed sampling effort within the aggregated block and disaggregated the results back to 1 km. For example, if two cells within the 10 × 10 km block each have 1 year of sampling effort, following disaggregation all cells in the 10 × 10 km block receive a sampling effort value of two. Sites with no anuran records were assigned a value of 0.01. The final sampling effort map is based on ~41,000 anuran records (Fig. S1), and we selected 10,000 background points from the study area with probability proportional to effort (sites with greater effort were more likely selected to describe the background area).

For contemporary distribution models, we extracted values for occurrence and background points for eight environmental variables representative of means, extremes and seasonality of precipitation and temperature (WORLDCLIM V. 1.4-release 3; Hijmans, Cameron, Parra, Jones, & Jarvis, 2005): mean annual temperature (bio1), temperature seasonality (bio4), mean temperature of warmest (bio10) and coldest quarter (bio11), total annual precipitation (bio12), precipitation seasonality (bio15), precipitation of wettest (bio16) and driest quarter (bio17). We selected this subset of variables to reflect environmental variation that is biologically informative for amphibians, while minimizing the number of correlated variables in the analysis (Fig. S1). To evaluate model performance, we set aside 25% of the occurrences at random and measured the area under the curve (AUC) of the receiver operating characteristic (ROC). The ROC plot reflects the fraction of correct presences (true positives) as a function of the fraction of incorrect absences (false negatives); however, in data sets such as ours where absence data are unavailable, the fraction of correct presences is plotted against the fraction of the study area predicted as present under each possible threshold. Although AUC estimates of performance can be misleading when comparing different modelling algorithms (Peterson, Papeş, & Soberón, 2008) or study areas (Lobo, Jiménez-Valverde, & Real, 2008), it is a suitable performance metric for our data set (presence-only, same modelling algorithm and study area). If model evaluation was positive (AUC > 0.8), we generated a final model using all available data. We evaluated the effects of changing the value of the regularization parameter and the allowed feature type classes on model performance using the ENMEVAL package (Muscarella et al., 2014) and found that the default parameters suggested by MAXENT

were reasonable for our study system (Fig. S1). The potential distributions of the taxa in historic time periods (see next section) are based on the final versions of the contemporary distribution models.

2.3 | Niche stability and connectivity through time

To extend niche models to historic climates, we used climate estimates for the last 120 kyr (Fuchs et al., 2013; Weber, VanDerWal, Schmidt, McDonald, & Shoo, 2014) and assumed that the estimated contemporary niche remained constant within this time period (Wiens et al., 2010). The climate surfaces were based on snapshots of 1–4 kyr intervals using the Hadley Centre Climate model (HadCM3; Singarayer & Valdes, 2010). Monthly temperature and precipitation anomalies were downscaled to 0.2 degrees using a bilinear spline and then to 0.0466667 degrees globally using a bicubic spline. Anomalies were then applied to current monthly climates given 125 m lower sea levels (Hijmans et al., 2005). Past sea levels were estimated as the consensus of several sources (Fleming et al., 1998; Fleming, 2000; Lea, Martin, Pak, & Spero, 2002; Milne, Long, & Bassett, 2005; R. A. Rohde unpublished data; Global Warming Art project http://en.wikipedia.org/wiki/File:Post-Glacial_Sea_Level.png, and <http://www.ncdc.noaa.gov/paleo/ctl/clisci100k.html#sea>), and climate surfaces for each time period were clipped to only include exposed land. We derived surfaces of mean annual temperature, temperature seasonality, mean temperature of the warmest and coldest quarters, mean annual precipitation, precipitation seasonality and precipitation of the wettest and driest quarters for each time slice. We deposited the geospatial bioclimatic layers for the current, middle Holocene, LGM and LIG in Dryad (<https://doi.org/10.5061/dryad.v576v>). The full set of layers is available upon request from coauthor JV. All analyses were conducted with the CLIMATES package (VanDerWal, Beaumont, Zimmermann, & Lorch, 2011) in R v 2.9.0.

We estimated stability of suitable climate for each species over the last 120 kyr using two approaches: static stability (Hugall, Moritz, Moussalli, & Stanicic, 2002), which does not consider dispersal between pixels, and dynamic stability (Graham, VanDerWal, Phillips, Moritz, & Williams, 2010), which employs a graph theoretic approach with estimates of dispersal rate to model how organisms track suitable climate conditions across time. With the dynamic stability approach a pixel is stable as long as pixels within the defined dispersal distance have suitable climate in adjacent time steps. For the static stability estimate, we summed the negative log of suitability through time for each pixel, and for the dynamic stability estimate

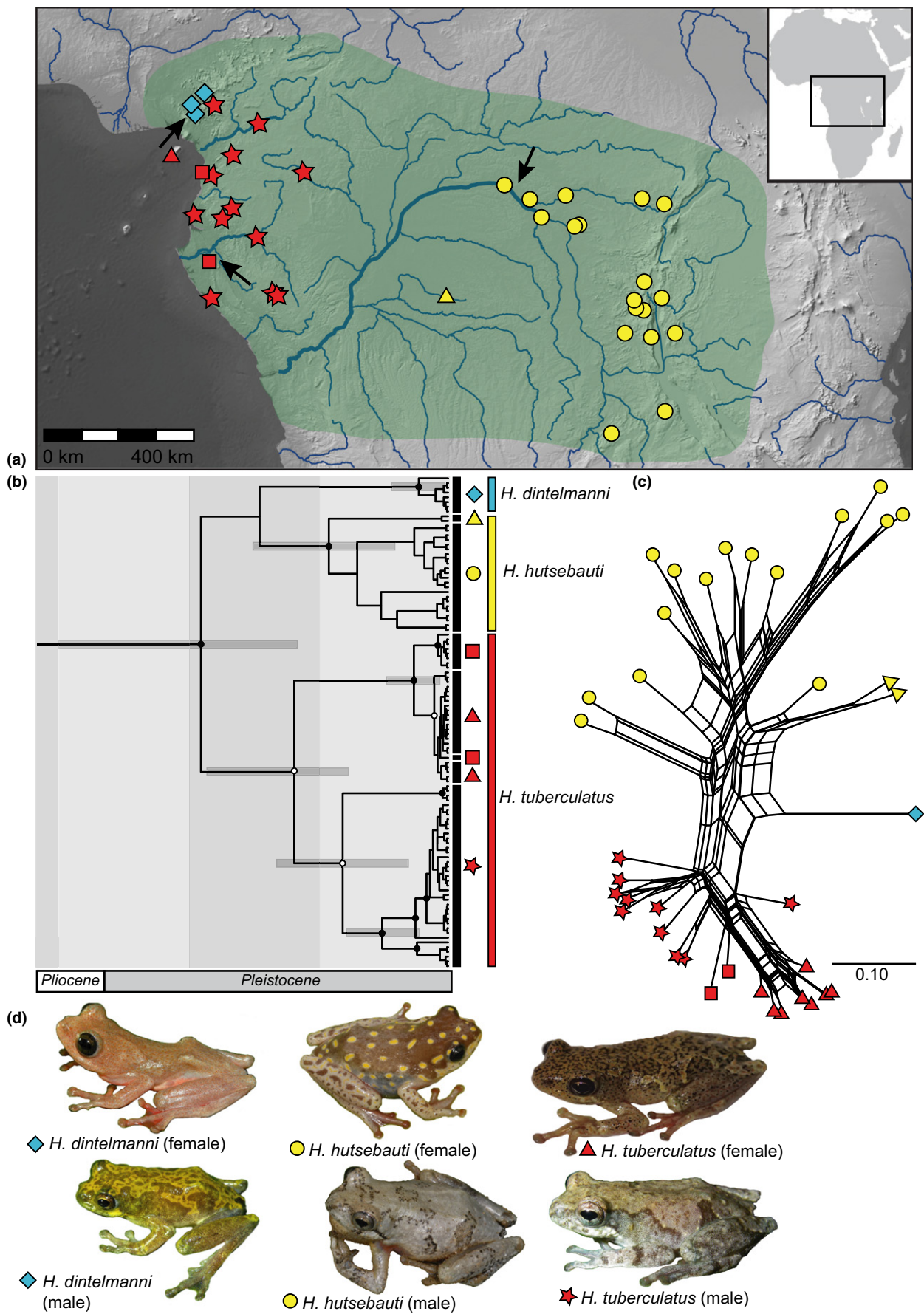


FIGURE 3 (a) Distribution of *Hyperolius tuberculatus* species complex sampling localities in Central Africa including Bioko Island. The approximate range is shown in green, and the type localities for *H. tuberculatus*, *H. dintelmanni* and *H. hutsebauti* are indicated with black arrows. (b) Mitochondrial (16S and *cytochrome b*) phylogeography; posterior probabilities >.95 are denoted by black dots, probabilities >.85 are denoted by white dots, and 95% highest posterior density intervals for divergence time estimates on well-supported nodes are indicated. The axis indicates geological epochs (Pliocene and Pleistocene) and time before present in increments of 1 million years. (c) Multilocus nuDNA networks generated using POFAD and SPLITSTREE. In all cases, samples are coded with shapes corresponding to mitochondrial lineages. The scale represents genetic distance equally weighted across loci. (d) Representative photographs of female and male coloration. Photograph credits: D. Portik, E. Greenbaum, B. Stuart, R. Bell

we followed Graham et al. (2010) with a 10 m/year dispersal rate. This dispersal rate is equivalent to 40 km or 8 pixels for 4 kya time intervals, which is a conservative estimate based on lifetime dispersal potential in frogs as well as large-scale biogeographic patterns in African frogs. We calculated stability surfaces using modified R scripts provided by S. Phillips (personal communication).

The contemporary distributions of the *Hyperolius tuberculatus* and *H. ocellatus* species complexes include the land-bridge island Bioko, while the *H. cinnamomeoventris* species complex is absent from the island; thus, we considered historic changes in coastline that may have facilitated or restricted dispersal between continental Africa and Bioko. We classified “mainland” and “island” as the current exposed area on continental Africa or on Bioko within the window $x_{\min} = 7.59693^\circ$, $x_{\max} = 10.35984^\circ$, $y_{\min} = 2.650173^\circ$, $y_{\max} = 5.079467^\circ$ and measured potential connectivity over the last 120 kyr using PATHMATRIX (McRae, 2006; McRae, Dickson, Keitt, & Shah, 2008) with the niche models for each time slice as conductance surfaces. PATHMATRIX implements circuit theory to calculate all possible movements between two areas (higher values of conductance correspond to higher potential dispersal), which better represents connectivity among populations than the least-cost path method (McRae & Beier, 2007). Effective conductance was scaled relative to the current size of Bioko Island (99 pixels).

2.4 | Genetic data collection and analysis

2.4.1 | Genetic data collection

We extracted total genomic DNA using DNeasy Blood & Tissue Kits (Qiagen Inc., Valencia, CA, USA). Two specimens were formalin-fixed (YPM A8062 and A8086), and we extracted DNA from these samples following a protocol developed by Cathy Dayton of the U.S. Fish and Wildlife Service (Methods S1). We amplified and sequenced one or two mitochondrial (mtDNA) fragments (16S and *cytochrome b*) and one to three nuclear (nuDNA) protein-coding genes (*cmcy*, *POMC*, *RAG1*) for each sample using published primers (Table S1–S3). Polymerase chain reactions (PCRs) were carried out in a final volume of 20 μ l containing: 20 ng template DNA, 1 \times Buffer, 0.2 μ M of each primer, 0.4 mM dNTP mix and 0.125 units of *Taq* DNA polymerase (Roche Diagnostics, Indianapolis, IN, USA). Amplification was carried out with an initial denaturation for 5 min at 94°C, followed by 35 cycles (60 s denaturation at 94°C, 60 s annealing at 42–55°C [Table S2], 60 s extension at 72°C) and a final extension at 72°C for 5 min. PCR products were purified using ExoSAP-IT (USB Corp.,

Cleveland, OH, USA), and sequenced using a BigDye Terminator Cycle Sequencing Kit v. 3.1 (Applied Biosystems, Foster City, CA, USA) on an ABI Automated 3730xl Genetic Analyzer (Applied Biosystems). DNA sequences were edited using SEQUENCHER v. 5.0.1 (Gene Codes Corp., Ann Arbor, MI, USA) and deposited in GenBank (Table S1). Sequences for 39 samples of the *H. cinnamomeoventris* complex (16S, *cytochrome b*, *cmcy*, *POMC* and *RAG1*) were collected in previous studies (Bell, Drewes, Channing, et al., 2015; Bell, Drewes, & Zamudio, 2015).

2.4.2 | Mitochondrial phylogeography

We included sequences from closely related taxa (Table S1) in preliminary analyses to ensure that each species complex represents a monophyletic group based on the current understanding of phylogenetic relationships in *Hyperolius* (Portik, 2015). These analyses revealed that a few samples included in Bell, Drewes, Channing, et al. (2015; AC 3096–3097, PM 35 and VGCD 1273–1274) are likely outside the *H. cinnamomeoventris* complex, and thus, they were not included in the present study. Sequences were aligned using CLUSTAL X v. 2.0.10 (Larkin et al., 2007). We used PARTITIONFINDER v. 1.1.0 (Lanfear, Calcott, Ho, & Guindon, 2012) to determine the best-fit nucleotide substitution models for each mtDNA locus (Table S3). For each species complex, we inferred the mtDNA phylogeny using Bayesian phylogenetic analyses implemented in BEAST v. 1.8.0 (Drummond, Suchard, Xie, & Rambaut, 2012). When we compared strict and uncorrelated lognormal relaxed molecular clock models in preliminary analyses, we found low rate variation among branches (the standard deviation parameters [ucl.d.stdev] of the uncorrelated lognormal relaxed clock analyses were close to zero); therefore, we used the strict clock model for the final analyses. We chose a constant size coalescent tree prior and obtained posterior distributions from two Markov chain Monte Carlo (MCMC) simulations, each run for 10 million generations and assessed convergence with TRACER v. 1.5 (Rambaut, Suchard, Xie, & Drummond, 2013). No fossils of hyperoliid frogs exist with which to calibrate divergence times; therefore, we applied a sequence divergence rate for the most stable and informative reference locus in our data set—*cytochrome b*—based on rates estimated for tropical bufonid frogs (0.80%–1.90% per Myr; Sanguila, Siler, Diesmos, Nuñez, & Brown, 2011). We selected a rate prior with a mean of 1.4% and a normal distribution (95% confidence interval of 0.8%–1.9%). The effective sample size for each parameter was well above 200, and simulations were repeated without sequence data to test the influence of priors on

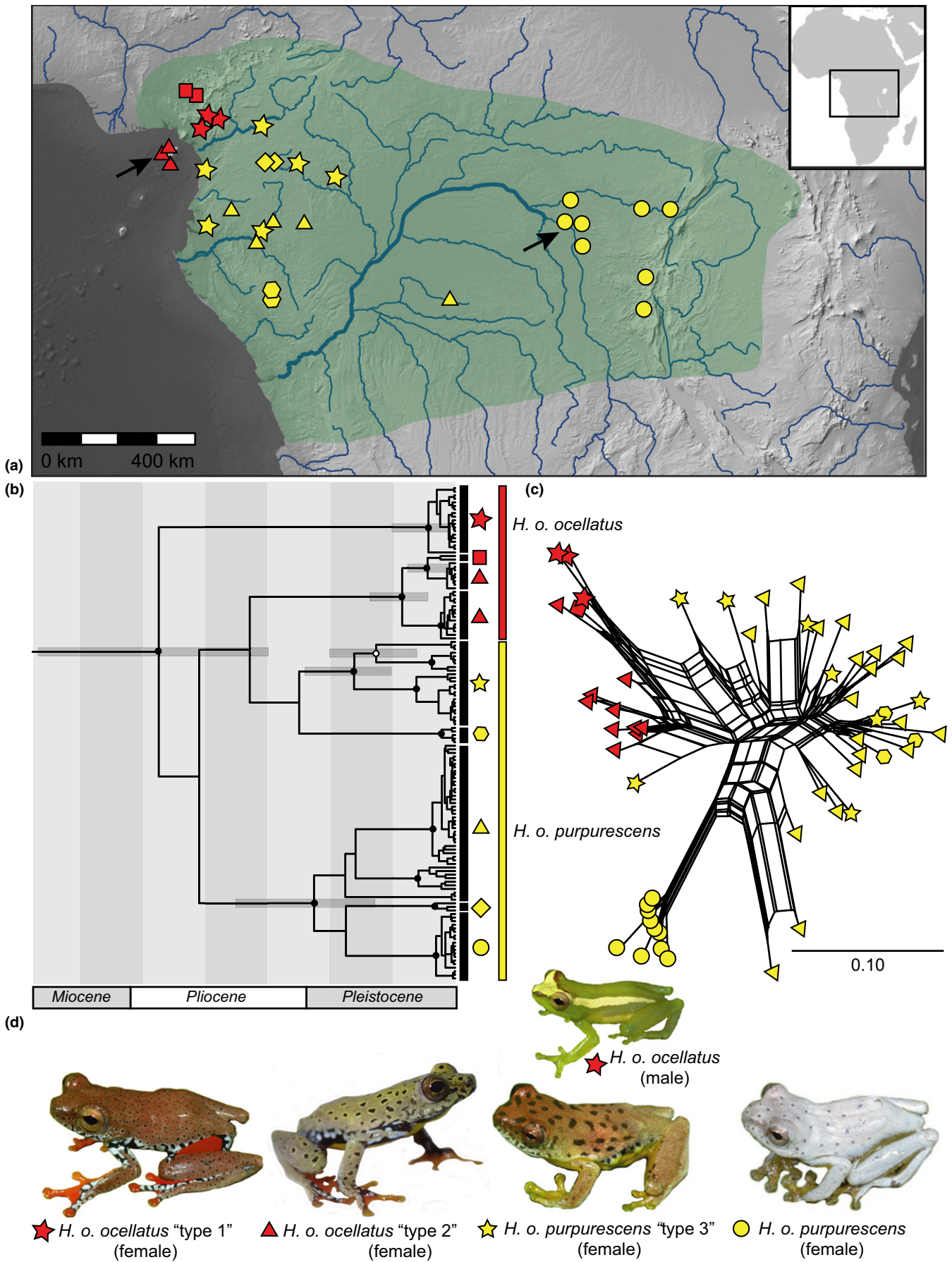


FIGURE 4 (a) Distribution of *Hyperolius ocellatus* species complex sampling localities in Central Africa including Bioko Island. The approximate range is shown in green, and the type localities for *H. o. ocellatus* and *H. o. purpurescens* are indicated with black arrows. (b) Mitochondrial (16S and *cytochrome b*) phylogeography; posterior probabilities $>.95$ are denoted by black dots, probabilities $>.85$ are denoted by white dots, and 95% highest posterior density intervals for divergence time estimates on well-supported nodes are indicated. The axis indicates geological epochs (Miocene, Pliocene and Pleistocene) and time before present in increments of 1 million years. (c) Multilocus nuDNA networks generated using POFAD and SPLITSTREE. In all cases, samples are coded with shapes corresponding to mitochondrial lineages. The scale represents genetic distance equally weighted across loci. (d) Representative photographs of distinct female colour morphs and male coloration. Photograph credits: D. Portik, P. McLaughlin, B. Stuart, E. Greenbaum

posterior distributions. We discarded the first 10% of trees as burn-in and combined the tree files from replicate runs using LOGCOMBINER prior to summarizing the posterior distribution of trees using TREEANNOTATOR.

2.4.3 | Differentiation at nuclear loci

Sequences were aligned using CLUSTAL X v. 2.0.10 (Larkin et al., 2007). We verified the absence of recombination within nuclear loci using the sum of squares method implemented in TOPALI 2 (Milne et al., 2009), resolved haplotypes for heterozygous individuals using PHASE v. 2.1 (Stephens, Smith, & Donnelly, 2001) implemented in DNASP v. 5.1 (Librado & Rozas, 2009) and generated individual gene trees for each locus using the neighbour-joining method in GENEIOUS v. 8.0.4 (Figs S2–S4).

We inferred population structure and assigned individuals to genetic populations with the Bayesian assignment program STRUCTURE v. 2.2.3 (Pritchard, Stephens, & Donnelly, 2000) using multilocus genotypes (phased haplotypes with the linkage model among SNPs within a locus). For each species complex, we only included individuals with data for at least two nuclear loci, which precluded including *H. dintelmanni* in the *H. tuberculatus* species complex analysis (only one sample met our missing data threshold). Preliminary analyses for the entire *H. cinnamomeoventris* species complex produced high variance in likelihood when K was greater than two. Thus, we split the samples for subsequent analyses following the deep divergence within the species complex: we ran analyses with K from one through five in *H. c. cinnamomeoventris* + *H. veithi*, and K from one through four in *H. c. olivaceus* + the island endemics. Preliminary analyses for the other two species complexes were more stable at higher values of K ; consequently, we ran analyses with K from one through four in the *H. tuberculatus* complex (*H. tuberculatus* + *H. hutsebauti*), and K from one through five in the *H. ocellatus* complex (*H. o. ocellatus* + *H. o. purpurescens*). For all analyses we ran ten iterations of each value of K with a burn-in of 1 million steps, MCMC length of 3 million steps, correlated allele frequencies and the admixture ancestry model. To determine the optimal number of genetic clusters in each data set, we used the method described by Evanno, Regnaut, and Goudet (2005).

To visually represent overall divergence patterns for samples with complete sequence data for the three nuclear genes, we used a multilocus, individual-based network approach. We used PAUP v. 4.0b (Swofford, 2003) to create genetic distance matrices between phased haplotypes at each locus using the HKY85 model (Hasegawa,

Kishino, & Yano, 1985). Using POFAD v. 1.03 (Joly & Bruneau, 2006), we combined individual locus matrices into one, multilocus distance matrix (equally weighted across loci). Finally, we constructed a genetic network of the multilocus distance matrix in SPLITSTREE v. 4.6 (Huson & Bryant, 2006) using the NeighborNet algorithm (Bryant & Moulton, 2004).

2.4.4 | Diversity and historical demography

For the distinct lineages we identified in each species complex through our mtDNA and nuDNA analyses, we calculated the number of variable sites and nucleotide diversity (θ_S , θ_π) in ARLEQUIN v. 3.1 (Excoffier, Laval, & Schneider, 2005). Using the combined mtDNA and nuDNA data set, we estimated changes in effective population size over time for the distinct lineages recovered within each species complex (based on mtDNA gene trees, the STRUCTURE analyses and SPLITSTREE networks of nuDNA distances) with the Extended Bayesian Skyline Plot approach (Heled & Drummond, 2008) implemented in BEAST2 v 2.4.5 (Bouckaert et al., 2014). We used PARTITIONFINDER v. 1.1.0 (Lanfear et al., 2012) to determine the best-fit nucleotide substitution models for the nuclear loci (Table S3) and applied the same mtDNA rate prior as described above. We obtained posterior distributions from two MCMC simulations, each run for 100 million generations and assessed convergence and the influence of priors as described above. We plotted the median and 95% central posterior density intervals of the demographic history of each lineage in R v 3.3.0 using BEAST2 scripts.

2.4.5 | Species tree estimation

Given that our focal species complexes have expansive geographic distributions and that current taxonomic designations do not necessarily reflect true diversity or evolutionary relationships, we used the multilocus coalescent model implemented in *BEAST (Heled & Drummond, 2010) to infer relationships within each species complex using the combined mtDNA and nuDNA data sets. The *BEAST approach makes the assumption that incomplete lineage sorting is the main source of inconsistency between gene trees and the underlying species tree and that there is no post-divergence gene flow between species. Thus, for each of the species complexes, we assigned individuals to putative species for the analysis following the distinct lineages recovered in the mtDNA gene trees, the STRUCTURE analyses and SPLITSTREE networks of nuDNA distances (Figures 2–4, Fig. S7; Table S3). We specified unlinked site, clock and tree models (the

TABLE 1 Number of unique occurrences for Ecological Niche Models (ENM), model fit (AUC) and per cent contribution of Bioclim variables for full-parameter ENMs for the *Hyperolius tuberculatus* complex (Ht), *H. ocellatus* complex (Ho), *H. c. olivaceus* (Hco.) and *H. c. cinnamomeoventris* (Hcc)

	Ht	Ho	Hco	Hcc
Unique localities (training/full)	43/57	35/46	15/20	34/45
AUC (train/test)	0.94/0.95	0.97/0.96	0.98/0.95	0.96/0.94
Variable (units)				
Annual precipitation bc12 (mm)	66.6	53.5	58.8	3.4
Precipitation of driest quarter bc17 (mm)	11.7	34.5	30.3	66.0
Temperature seasonality (SD*100) bc04	11.3	1.7	0.7	16.7
Mean temperature of coldest quarter bc11 (°C)	7.7	5.1	0.7	8.0
Precipitation seasonality (coefficient of variation) bc15	2.1	0.7	9.3	5.9
Annual mean temperature bc01 (°C)	–	2.4	0.2	–
Mean temperature of warmest quarter bc10 (°C)	–	2.0	–	–
Precipitation of wettest quarter bc16 (mm)	0.6	–	–	–

tree model for mtDNA loci was linked), a Yule process tree prior, and a strict molecular clock model with the same mtDNA rate prior as described above. We obtained posterior distributions from two MCMC simulations, each run for 200 million generations, and assessed convergence and the influence of priors as described above. We discarded the first 10% of trees as burn-in and combined the tree files from replicate runs using LOGCOMBINER prior to summarizing the posterior distribution of trees using TREEANNOTATOR.

3 | RESULTS

3.1 | Ecological niche modelling, niche stability and connectivity through time

Niche models for the *Hyperolius tuberculatus* complex, the *H. ocellatus* complex, *H. c. olivaceus* and *H. c. cinnamomeoventris* had a reasonable performance with AUC values ranging from 0.94 (*H. tuberculatus* complex) to 0.98 (*H. c. olivaceus*; Figure 1, Table 1, Fig. S3). Precipitation-related variables, specifically annual precipitation, precipitation seasonality and precipitation of the driest quarter, were critical in all four models (Table 1); relative occurrence rate was higher in areas with more than 1,500 mm of annual precipitation. *Hyperolius c. cinnamomeoventris*, however, occupies drier environments (down to 500 mm of annual precipitation) and occurs in areas with relatively high seasonality and a dry quarter with almost no rain, whereas the *H. tuberculatus* complex, *H. ocellatus* complex and *H. c. olivaceus* occur in sites with lower seasonality in precipitation and usually some rain in the driest quarter.

Estimates of climatic stability based on the static and dynamic stability surfaces were qualitatively similar with the dynamic stability models producing slightly larger and more contiguous stable areas (Figure 1, Fig. S5). The ENMs identified similar predicted suitable and stable climates in the *H. tuberculatus* and *H. ocellatus* complexes that included moderate-to-high suitability across the Congo Basin with the greatest climatic stability in the Lower Guinean forests

(including Bioko Island, Fig. S6) and smaller pockets of stability in the Congolian forests (Figure 1). For *H. c. olivaceus*, the ENMs recovered suitable and stable climates in the Lower Guinean forests with the highest suitability centred in Gabon (Figure 1). Although stable climates were predicted farther north in coastal Cameroon, the present known range of *H. c. olivaceus* does not extend that far north. By contrast, the ENMs recovered suitable and stable climates for *H. c. cinnamomeoventris* across much of the Congolian forests and stopping short of the Lower Guinean forests (Figure 1). Finally, maximum connectivity for the *H. tuberculatus* and *H. ocellatus* complexes between Bioko Island and continental Africa occurred at the LGM (21 kya and 22 kya, respectively) and remained high throughout most of the 15–72 kyr period (Figure 5, Fig. S7). By contrast, connectivity for *H. c. cinnamomeoventris* and *H. c. olivaceus* remained low throughout the last 120 kyr (Figure 5, Fig. S7).

3.2 | Mitochondrial phylogeography

The mtDNA phylogenies of the three species complexes revealed varying levels of divergence across the Lower Guineo-Congolian forests. In the *Hyperolius cinnamomeoventris* species complex, we recovered Late Miocene divergence between *H. c. olivaceus*, the island endemics, and a clade comprised of *H. c. cinnamomeoventris* and *H. veithi* (Figure 2b). *Hyperolius c. olivaceus* is restricted to the Lower Guinean forests and is comprised of two lineages that diverged in the early Pleistocene. By contrast, the *H. c. cinnamomeoventris* clade spans the Congolian forests and consists of five lineages (including *H. veithi*) with episodes of further divergence throughout the Pliocene and Pleistocene. In the *H. tuberculatus* complex, we recovered three distinct lineages with divergence across the Lower Guineo-Congolian forests spanning the Pliocene-Pleistocene transition (Figure 3b). We found that *H. dintelmanni* is distinct from adjacent populations of *H. tuberculatus* in Cameroon, *H. hutsebauti* north of the Congo River is nested within a lineage of eastern *H. tuberculatus* populations, and *H. tuberculatus* from Bioko Island (red triangles; Figure 3) is nested within a clade from coastal Cameroon and Gabon

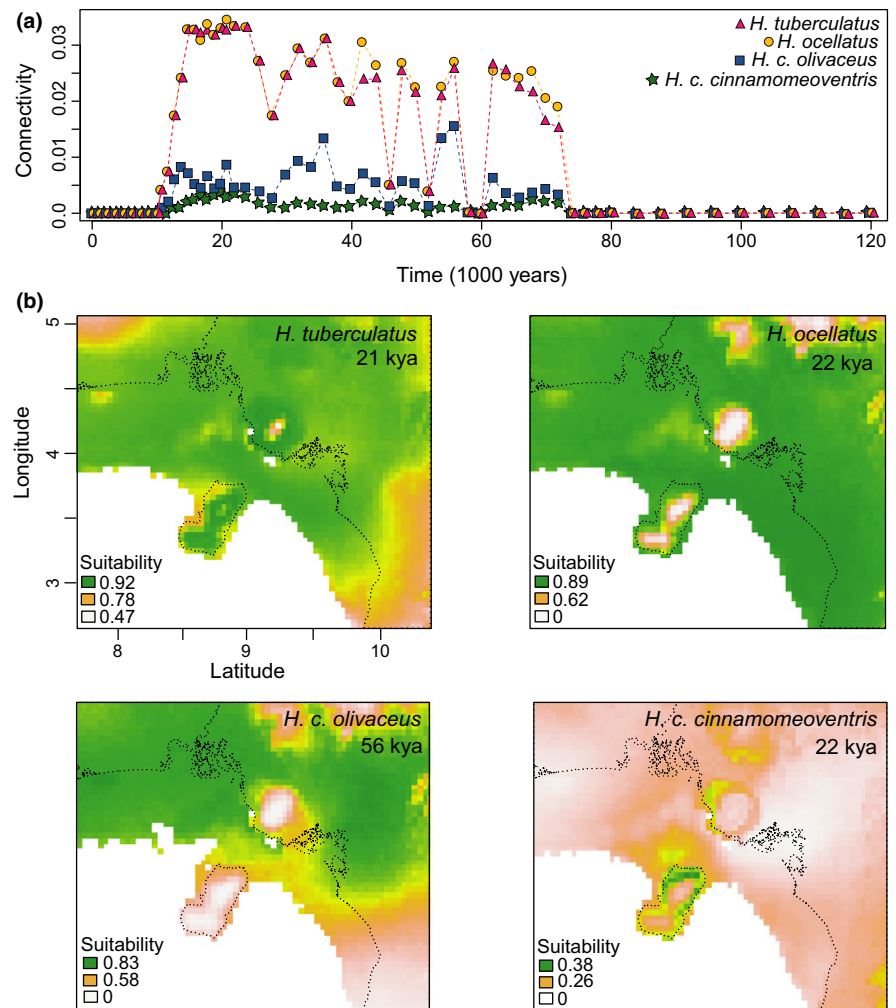


FIGURE 5 (a) Estimates of potential connectivity between Bioko Island and the African continent for the *Hyperolius tuberculatus* complex, *H. ocellatus* complex, *H. c. olivaceus* and *H. c. cinnamomeoventris* estimated using PATHMATRIX with the niche models for each time slice as conductance surfaces. Higher values of conductance correspond to higher potential dispersal. Connectivity (effective conductance) is scaled relative to the contemporary size of Bioko Island (99 pixels) (b) Distribution of climatic suitability for the *H. tuberculatus* complex, *H. ocellatus* complex, *H. c. olivaceus* and *H. c. cinnamomeoventris* at the respective periods of peak potential connectivity between Bioko Island and the African continent. Note the differences in scale and time period between panels

(red squares; Figure 3). Finally, in the *H. ocellatus* complex we found extensive phylogeographic structure across the Lower Guineo-Congolian forests with divergence throughout the Pliocene and Pleistocene. We identified three distinct mtDNA lineages in Cameroon that correspond to the three regional morphotypes (Figure 4); however, populations attributed to *H. o. purpureus* across the species complex range consist of several distinct lineages that may be paraphyletic with respect to *H. o. ocellatus*. Likewise, populations of *H. o. ocellatus* from Bioko Island (red triangles; Figure 4) form two distinct subclades that occur in sympatry on the island and are paraphyletic with respect to populations in southwest Cameroon (red squares; Figure 4).

3.3 | Differentiation at nuclear loci

The vast majority of haplotypes were resolved computationally with probabilities of 0.51 or greater (>87%). Sets of haplotypes with low probabilities were due to singleton or low frequency SNPs for which phasing errors likely have very little influence on our estimates of genetic structure in the STRUCTURE analyses or genetic distance in the SPLITSTREE networks; thus, we retained the set of haplotypes with the highest probability even if it was below 0.51. For the

H. cinnamomeoventris and *H. tuberculatus* species complexes, the STRUCTURE analyses and multilocus distance networks were largely congruent with the mtDNA phylogenies. The *H. cinnamomeoventris* species complex was comprised of five demes (*H. c. olivaceus*, the island endemics, *H. veithi*, and distinct eastern and western populations of *H. c. cinnamomeoventris*; Fig. S7). In the *H. tuberculatus* species complex, *H. dintelmanni* was not included in the analyses due to small sample size and STRUCTURE recovered two demes corresponding to western populations of *H. tuberculatus* and eastern populations of *H. tuberculatus* + *H. hutsebauti* (Fig. S3). In both species complexes, distinct mtDNA lineages that occur in near sympatry were also differentiated at nuclear loci (Figures 2 and 3, Figs S2 and S3). Although we recovered extensive mtDNA structure in the *H. ocellatus* species complex, the STRUCTURE analyses of nuDNA recovered two demes largely corresponding to *H. o. ocellatus* and *H. o. purpureus* (Fig. S7). While the distinct mtDNA lineage of *H. o. purpureus* in the eastern part of the range (yellow circles) was differentiated from western lineages in the SPLITSTREE network, the remaining mtDNA lineages in the western part of the range (yellow stars, hexagons, diamonds and triangles) were not differentiated from one another at nuclear loci (Figure 4, Fig. S4). Furthermore, the allopatric type 1 and type 2 morphotypes in Cameroon (red symbols;

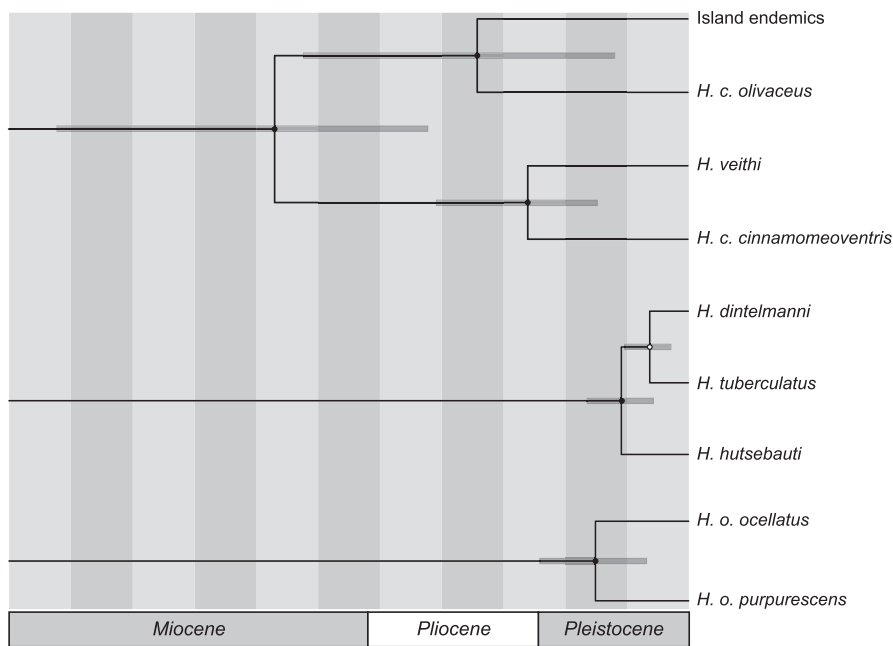


FIGURE 6 *BEAST species tree inference for combined mtDNA and nuDNA haplotypes collected from the *Hyperolius cinnamomeoventris* species complex, the *H. tuberculatus* species complex and the *H. ocellatus* species complex. Posterior probabilities $>.95$ are denoted by black dots, probabilities $>.90$ are denoted by white dots, and 95% highest posterior density intervals for divergence time estimates are indicated

Figure 4) and mtDNA subclades on Bioko Island (red triangles; Figure 4) were undifferentiated at nuclear loci (Fig. S4).

3.4 | Historical demography

Given the small sample sizes for the geographically restricted lineages in two of the species complexes—*H. veithi* and the island endemics (*H. cinnamomeoventris* complex) and *H. dintelmanni* (*H. tuberculatus* complex)—we estimated changes in effective population size over time for the primarily western versus eastern lineages within each complex (Fig. S8). Across all three species complexes, the western lineages (*H. c. olivaceus*, western *H. tuberculatus* and *H. o. ocellatus*) exhibited smaller and more stable population sizes through time with moderate signatures of recent expansion in western *H. tuberculatus* and 95% HPD intervals in *H. c. olivaceus* and *H. o. ocellatus* that include constant size (Fig. S8). By contrast, the eastern lineages (*H. c. cinnamomeoventris*, eastern *H. tuberculatus* + *H. hutsebauti* and *H. o. purpurescens*) exhibited larger population sizes with substantial increases and/or decreases in population size over time (Fig. S8).

3.5 | Species tree estimation

For the *H. cinnamomeoventris* species complex, we assigned samples from the mainland to operational species units following the mtDNA and multilocus nuDNA analyses (*H. c. cinnamomeoventris*, *H. c. olivaceus* and *H. veithi*). We grouped samples of the island endemic species (*H. thomensis*, *H. mollerii* and *H. drewesi*) into a single operational species unit because few sites in our nuDNA data set were variable between these recently diverged island species. Analyses with *H. c. cinnamomeoventris* split into eastern and western lineages (blue and yellow symbols in Figure 2) did not reach convergence after 200 million generations so we grouped these samples into a

single operational species unit. The species tree reconstruction strongly supported *H. c. cinnamomeoventris* and *H. veithi* as sister lineages and *H. c. olivaceus* and the island endemics as sister lineages (Figure 6). For the *H. tuberculatus* complex, we assigned samples to three operational species units following the mtDNA and multilocus nuDNA analyses (*H. dintelmanni*, western *H. tuberculatus* and eastern *H. tuberculatus* + *H. hutsebauti*; distinct colours in Figure 3). The species tree reconstruction supported western *H. tuberculatus* and *H. dintelmanni* as sister lineages in this recent radiation (Figure 6). For the *H. ocellatus* complex, the multilocus nuDNA analyses recovered two lineages (*H. o. ocellatus* and *H. o. purpurescens*; distinct colours in Figure 4); thus, we assigned samples to these two operational species units to obtain divergence time estimates that were comparable with the other species complexes (Figure 6). Across all three species complexes, the point estimates of divergence in the species tree analyses were more recent than those estimated in the mtDNA analyses; however, divergence estimates within the *H. cinnamomeoventris* complex predated those of the *H. tuberculatus* and *H. ocellatus* complexes in both sets of analyses.

4 | DISCUSSION

4.1 | Idiosyncratic responses to climate-driven vicariance across Central Africa

Our analyses of multilocus sequence data demonstrate both temporal and spatial heterogeneity in patterns of diversification among sympatric reed frog species across the Lower Guineo-Congolian forests. Factors such as environmental heterogeneity and ecological interactions can limit the geographical extent of species ranges, yet species distributions are often largely determined by the limits of a species' physiological tolerance and spatial variation in climate

(Chown et al., 2010). Our estimates of current climatic suitability and climatic stability through time indicate that differences in climatic niche may partly explain idiosyncratic patterns of diversification among our three focal species complexes. We acknowledge that our divergence date estimates rely on a number of assumptions (e.g., substitution rate is equal to the mutation rate for within-species inferences) and that these approaches tend to overestimate divergence dates between recently diverged lineages (Herman & Searle, 2011). Even with these limitations, our divergence date estimates based on the mtDNA-only data set and the combined mtDNA and nuDNA data sets enable us to propose a general timeframe for divergence events and demonstrate variation in divergence times among the species complexes (e.g., non-overlapping 95% HPD intervals).

The *Hyperolius cinnamomeoventris* species complex is broadly distributed in both forest and bushland habitats across Central Africa; however, we recovered Late Miocene divergence between *H. c. cinnamomeoventris* and *H. c. olivaceus* across the boundary of the Lower Guinean and Congolian forests in Gabon and Republic of the Congo (Figure 2). This region appears as largely contiguous lowland rainforest habitat, yet *H. c. olivaceus* is restricted to sites with low seasonality, while *H. c. cinnamomeoventris* occupies drier environments with relatively high seasonality. Consequently, the climatic stability models demarcate distinct regions of climatic suitability for *H. c. olivaceus* and *H. c. cinnamomeoventris* throughout the variable climates of the last 120 kyr, and this demarcation appears to have persisted since the Late Miocene. Thus, this pattern of allopatric divergence coupled with marked divergence in environmental niche is consistent with the “vanishing refuge” model of speciation wherein habitat fragmentation and exposure to new environments result in closely related lineages occupying adjacent, contrasting habitats (Damascono, Strangas, Carnaval, Rodrigues, & Moritz, 2014; Vanzolini & Williams, 1981). Furthermore, the estimated divergence between the two lineages coincides with periods of aridification in the Miocene that are attributed with driving diversification of predominantly forest-restricted plant and animal lineages into drier savannah habitats (Holstein & Renner, 2011; Johnston & Anthony, 2012).

Relative to the *H. cinnamomeoventris* species complex, divergences in the *H. tuberculatus* and *H. ocellatus* complexes are more recent (Pliocene to Pleistocene), and these frogs are restricted to forest habitats with low seasonality. Correspondingly, the climatic suitability models recover similar suitable climates for these species complexes with the highest stability centred in the Lower Guinean forests. Although current distributions of both species complexes span the Congo Basin, our estimates of climatic suitability and stability over the last 120 kyr indicate that these populations likely experienced several periods of contraction and expansion throughout the variable climates of the Pliocene and Pleistocene (Hardy et al., 2013; Plana, 2004). Genetic diversity in both the *H. tuberculatus* and *H. ocellatus* complexes is concentrated in the Lower Guinean forests and the Extended Bayesian Skyline Plots reveal smaller and more stable populations in this region relative to the Congo Basin lineages. These patterns are consistent with long-term lineage persistence and

high climatic stability in Lower Guinean forests (Born et al., 2011; Dauby, Duminil, et al., 2014; Faye, Deblauwe, Mariac, & Richard, 2016; Leaché & Fujita, 2010; Plana, 2004; Quéroutil et al., 2003), versus fluctuating and more fragmented stability across the Congo Basin (Jacquet et al., 2015; Johnston & Anthony, 2012; Nicolas et al., 2011; Tosi, 2008).

Although our modest molecular data set limits strong inferences based on divergence time estimates, we consistently recover more pronounced phylogeographic structure in the *H. ocellatus* complex than in the *H. tuberculatus* complex. *Hyperolius ocellatus* breeds in small rainforest streams and swamps, and is rarely found outside of forest habitats (Amiet, 2012), whereas frogs in the *H. tuberculatus* complex breed in forest clearings and swamps, and are more tolerant of edge or open forest habitats (Amiet, 2012). These differences in ecological breadth between the species may buffer the effects of habitat fragmentation in *H. tuberculatus* relative to *H. ocellatus* (Rodríguez et al., 2015). The species complexes also differ in body size: frogs of the *H. ocellatus* complex are sexually dimorphic in size (males ~20 mm snout-vent length [SVL], females ~30 mm SVL; Amiet, 2012), whereas males and females in the *H. tuberculatus* complex are similar in size (~30 mm SVL; Amiet, 2012). Over ~90% of frog species display sexual dimorphism in body size and this variation is typically attributed to selection for increased fecundity when females are larger (Salthe & Duellman, 1973) or strong sexual selection when males are larger (Shine, 1979). Thus, differences in selection related to fecundity and/or mating system, as well as body size-associated dispersal ability (Pabijan, Wollenberg, & Vences, 2012; Wollenberg, Vieites, Glaw, & Vences, 2011), may also be contributing to the differences in phylogeographic structure we recovered. Studies in co-distributed rainforest trees, understory plants and lianas in Lower Guinean forests also recover varied responses to proposed barriers in this region (Budde, González-Martínez, Hardy, & Heuertz, 2013; Dauby, Duminil, et al., 2014; Faye et al., 2016; Heuertz et al., 2014; Ley et al., 2014). This growing literature indicates that accounting for species traits related to ecological breadth, dispersal and mating system will be essential for understanding shared phylogeographic patterns in this region. In addition, more extensive geographic sampling in montane and lowland sites throughout Cameroon and Gabon coupled with methods that explicitly account for changes in population size and gene flow may more rigorously detect differences in forest species' responses to a shared climatic history (Bell et al., 2012; Dasmahapatra, Lamas, Simpson, & Mallet, 2010; Hickerson, Stahl, & Lessios, 2006; Leaché, Crews, & Hickerson, 2007).

Despite marked differences among the *H. ocellatus*, *H. tuberculatus* and *H. cinnamomeoventris* species complexes in the geographic extent and temporal estimates of divergence, we recover a shared pattern of intermittent moderate-to-high climatic suitability across the Congo Basin in the last ~120 kyr (Figure 1, Fig. S7) and mtDNA clades that extend across this expansive region originate at the Pliocene-Pleistocene transition (*H. c. cinnamomeoventris*, *H. o. purpureus* and the *H. tuberculatus* complex; Figures 2–4). These patterns are consistent with studies in rainforest trees (Couvreur

et al., 2008), rodents (Bryja et al., 2017; Nicolas et al., 2011) and primates (Tosi, 2008), and support the hypothesis that genetic exchange across the Congo Basin during more humid periods, followed by divergence during arid periods, has shaped patterns of regional diversity (Fjelds  & Lovett, 1997; Tosi, 2008). Populations of *H. c. cinnamomeoventris* east and west of the Congo Basin are strongly differentiated in both the mtDNA and nuDNA data sets (blue and yellow symbols; Figure 2, Fig. S7), which is consistent with allopatric divergence on either side of the Congo Basin. Further sampling across the northern Congo Basin is needed to confirm that these lineages diverged in allopatry (versus simple isolation by distance) and if so, assess whether eastern and western lineages persist or become obscured when they come into secondary sympatry in the Congo Basin (Holstein & Renner, 2011). Likewise, we find distinct mtDNA lineages in the centre of the Congo Basin in the *H. ocellatus* and *H. tuberculatus* complexes (yellow triangles, Figures 3 and 4) that coincide with the distribution of the recently described *H. veithi* in the *H. cinnamomeoventris* species complex (Figure 2), but this pattern may also be an artefact of isolation-by-distance and our discontinuous sampling. More extensive sampling across the central Congo Basin will likely reveal additional cryptic diversity within each species complex and provide greater insight into the temporal and spatial dynamics of lineage diversification in this region.

4.2 | Rivers, lineage divergence and phenotypic variation in Central African *Hyperolius*

The distributions of our focal species complexes span three major rivers (the Congo, the Ogoou  and the Sanaga) that are barriers to dispersal in many mammal and understory bird species across the Guineo-Congolian forest (Anthony et al., 2007; Hassanin et al., 2015; Huntley & Voelker, 2016; Mitchell et al., 2015; Nicolas et al., 2011; Qu rouil et al., 2003; Telfer et al., 2003). Although we recovered extensive phylogeographic structure in each species complex, these regional clades typically include localities on either side of the Sanaga, Ogoou  and Congo rivers and these regional clades also span two or more of the major river drainages. This pattern indicates that broad-scale phylogeographic structure in these frogs does not correspond to Central African hydrobasins and that rivers are likely not significant barriers to dispersal. In particular, although the Congo River is the proposed barrier between *H. tuberculatus* and *H. hutsebauti* in the Democratic Republic of the Congo (Laurent, 1956, 1976), our results suggest that divergence in this species complex is not delineated by the Congo River. Our data are consistent, however, with the Sanaga River serving as the boundary between *H. o. ocellatus* and *H. o. purpureus* in Cameroon (Laurent, 1943; Perret, 1975). Patterns of divergence across the Sanaga may be confounded by the historical presence of lowland rainforest climatic refugia on either side of the river (Dauby, Duminil, et al., 2014; Dauby, Hardy, et al., 2014; Droissart et al., 2011). This region had high predicted climatic suitability in our ENMs (Figure 1); consequently, patterns of phylogeographic structure in the *H. ocellatus* species complex may

be difficult to interpret with respect to these coinciding biogeographic features.

We recovered a wide range of divergence times and distinct lineages among our focal taxa, many of which may reflect incipient species. In particular, the result that regional variation in female coloration across the *H. ocellatus* complex corresponds to distinct mtDNA lineages is especially intriguing. Lineages that diverged in response to earlier climatic or geologic processes (e.g., Pliocene or Late Miocene) are expected to exhibit stronger postzygotic isolation than those that formed in response to more recent (Pleistocene) events (Avise, 2000; Singhal & Moritz, 2013; Weir & Price, 2011). Likewise, divergence in phenotypic traits involved in social signalling is also expected to scale with divergence in geographic isolation (Winger & Bates, 2015). Although the function of colour polymorphism and sexual dichromatism in reed frogs is unknown, these traits may be relevant for species recognition and/or mate choice. Alternatively, colour polymorphism may reflect varying selection processes including differences in predation regimes, as occurs with poison-dart frogs (Brown, Maan, Cummings, & Summers, 2010), or alternate reproductive strategies, as demonstrated in the rock-paper-scissors system in side-blotched lizards (Sinervo & Lively, 1996). These selective mechanisms can result in rapid phenotypic evolution (Corl, Davis, Kuchta, & Sinervo, 2010) and/or accelerated speciation rates (Hugall & Stuart-Fox, 2012). Thus, the spectrum of divergence times across our focal taxa, regions of secondary contact between previously isolated lineages, extensive colour polymorphism, and variation in sexual size dimorphism and dichromatism present a rich comparative framework in which to investigate reproductive isolation and phenotypic divergence in Central African *Hyperolius*.

4.3 | Marine incursions and population divergence on the land-bridge island Bioko

Although the *H. cinnamomeoventris* complex is widely distributed across Central Africa, none of the lineages occur on Bioko Island, and our estimates of connectivity indicate that low climatic suitability between Bioko and the continent may have precluded colonization when the land bridge was exposed (Figure 5). By contrast, *H. tuberculatus* and *H. o. ocellatus* occur on Bioko and niche models for the *H. tuberculatus* and *H. ocellatus* species complexes reveal high connectivity between Bioko and the continent between 14 and 70 kya. As in previous phylogeographic studies of Bioko Island reptiles and amphibians (Barej et al., 2014; Leach  & Fujita, 2010; Leache, Fujita, Minin, & Bouckaert, 2014), we find moderate genetic divergence between mainland and island populations of *H. o. ocellatus* and *H. tuberculatus*, indicating that gene flow between Bioko and the continent is not ongoing. In both species complexes, we recover Late Pleistocene origins for the Bioko Island populations, but with two distinct mtDNA clades in *H. o. ocellatus* (TMRCA 30–290 kya, and 90–460 kya) and one in *H. tuberculatus* (40–210 kya). Again, our modest molecular data set limits strong inferences based on divergence time estimates; however, the ages of the younger *H. o. ocellatus* clade and *H. tuberculatus* clade are roughly coincident with the period of high connectivity we recover

in the historic climatic suitability models (Figure 5a) and indicate that dispersal across the land bridge has likely occurred multiple times in the island's 3 Myr old history. In addition, in both *H. o. ocellatus* and *H. tuberculatus* we find that adjacent continental populations are nested within Bioko Island lineages (Figures 3 and 4), which may reflect "reverse colonization" from Bioko to the continent during these periods of connectivity (Bellemain & Ricklefs, 2008). Reed frogs colonized two oceanic islands in the Gulf of Guinea (Príncipe and São Tomé) via rafting (Bell, Drewes, Channing, et al., 2015) and it is possible that *H. o. ocellatus* and *H. tuberculatus* colonized Bioko Island via similar sweepstakes colonization events; however, relatively high genetic diversity of the island populations and recent (Late Pleistocene) population divergence from the mainland are more consistent with vicariance due to marine incursions rather than multiple overseas dispersal events.

Bioko harbours multiple mtDNA lineages of *H. o. ocellatus* that are not differentiated at nuDNA and a single mtDNA lineage of *H. tuberculatus*, which mirrors the divergence pattern we recovered in continental Africa and may further reflect how habitat specificity and dispersal ability shape species' responses to shared biogeographic barriers. The species complexes also differ with respect to the geographic location of mainland populations most closely related to those on Bioko Island. *Hyperolius o. ocellatus* on Bioko are most closely related to mainland populations in southwestern Cameroon (red squares, Figure 4), similar to the pattern recovered in African forest geckos (*Hemidactylus fasciatus*; Leaché & Fujita, 2010; Leache et al., 2014). By contrast, Bioko populations of *H. tuberculatus* are most closely related to mainland populations in coastal Cameroon and Gabon (red squares, Figure 3), which is similar to the pattern recovered in African clawed frogs (*Xenopus calcaratus*, *X. allofraseri*; Evans et al., 2015). Differences in the timing of divergence between island and mainland populations of *H. tuberculatus* and *H. o. ocellatus*, as well as the geographic locations of the most closely related mainland populations, reinforce the conclusion that marine incursions are not the only factor restricting dispersal between Bioko and the continent. Instead, the composition of habitats connecting Bioko to the rest of the continent when sea levels retreat and species-specific differences in dispersal potential through these habitats likely mediate gene flow across the land-bridge for island residents and may preclude island colonization for some continental species altogether.

4.4 | Implications for reed frog taxonomy

We recovered multiple distinct evolutionary lineages within the continental distribution of the *H. cinnamomeoventris* complex that correspond to ecologically and phenotypically distinct populations. *Hyperolius veithi*, *H. c. cinnamomeoventris* and *H. c. olivaceus* are differentiated in both mtDNA and nuDNA are strongly supported as distinct lineages in our species tree analysis, and *H. c. cinnamomeoventris* and *H. c. olivaceus* occupy different environmental niches. Furthermore, we find no evidence for introgression between these three lineages even though we collected *H. c. cinnamomeoventris* within 10 km of *H. c. olivaceus* and *H. veithi*; thus, we recommend

recognizing each of these lineages as full species. The type locality of *H. olivaceus* Buchholz & Peters, 1876 (Lambaréné, Gabon), which was considered a subspecies of *H. cinnamomeoventris* by Laurent (1943), is among the localities for *H. c. olivaceus* in this study. Given our results, we elevate *H. c. olivaceus* to *H. olivaceus* (i.e., from the rank of subspecies to species). Our results indicate that *H. c. cinnamomeoventris* exhibits substantial cryptic diversity and is paraphyletic with respect to *H. veithi*; however, we refrain from taxonomic revision within this lineage pending additional sampling. Given our concordant results among mtDNA and nuDNA analyses, we refer the eastern lineages of *H. tuberculatus* to *H. hutsebauti*; however, resolving the geographic boundary between the two species will require more continuous sampling across the Congo Basin.

ACKNOWLEDGEMENTS

For fieldwork in Gabon we thank the CENAREST, ANPN and the Direction de la Faune et des Aères Protégées for permits, the Wildlife Conservation Society Gabon Program and Organisation Ecotouristique du Lac Oguemoué for logistical support, and N. Emba-Yao, F. Moiniyoko, B. Hylayre, E. Ekomy, A. Dibata, T. Ogombet, U. Eyagui, P. Endazokou, for assistance in the field. For fieldwork in Equatorial Guinea we thank Universidad Nacional de Guinea Equatorial and Jose Manuel Esara Echube for permits, the Bioko Biodiversity Protection Program, ExxonMobil Foundation, and Mobil Equatorial Guinea Inc. for logistical support, and A. Fertig, B. Miles, and D. Matute for assistance in the field. For fieldwork in Cameroon, we thank the Ministry of Scientific Research and Innovation and the Ministry of Forestry and Wildlife for permits, and O. Kopecky, B. Freiermuth, N.L. Gonwouo, G. Jongsma, M.T. Kouete and L. Scheinberg for assistance in the field. For fieldwork in the Republic of Congo, we thank J. Gaugris of Flora Fauna & Man, Ecological Services Ltd for logistical support and the Groupe d'Etude et de Recherche sur la Diversité Biologique for permits. Fieldwork by ZTN in Democratic Republic of the Congo was supported by the Parc Marin des Mangroves, ICCN (M. Collet) and the Belgian National Focal Point to the Global Taxonomy Initiative. Fieldwork in Angola was supported by P. vas Pinto. Fieldwork by EG in Democratic Republic of the Congo was supported by the Centre de Recherche en Sciences Naturelles, ICCN, Mwenebatu M. Aristote and Wandeghe M. Muninga. For fieldwork in Rwanda, we thank the Rwandan Development Board for permits. We thank K. Jackson, D. Mulcahy, L. Scheinberg, C. Spencer, J. Rosado, G. Watkins-Colwell, J. Vindum and A. Wynn for providing access to tissue samples in their care, M. Hydeman for assistance in the molecular laboratory, S.B. Reilly for computational resources, and H.W. Greene, R.G. Harrison, J.I. Lovette and five anonymous reviewers for comments that improved the manuscript. Funding was provided by the Explorer's Club, American Philosophical Society, Sigma Xi, Society of Systematic Biologists, Mario Einaudi Center for International Studies, Cornell Graduate School, Andrew W. Mellon Foundation, EEB Paul P. Feeny Fund, EEB Paul Graduate Fellowship and a University of California President's Postdoctoral Fellowship (to

RCB); Museum of Comparative Zoology Herpetology Division at Harvard University (to RCB & BLS); the BIOTA projects of the Federal Ministry of Education and Research (BMB+F, Germany to SL and MOR); the US National Science Foundation (DEB-1309171 to RCB, DEB-1202609 to DCB and DEB-1145459 to EG); the National Geographic Society (8556-08 to EG, 8868-10 to RCB); the California Academy of Sciences (to DCB); the Percy Sladen Memorial Fund, IUCN/SSC Amphibian Specialist Group, K. Reed, M.D., the Department of Biology at Villanova University and the University of Texas at El Paso (to EG); the Czech Science Foundation (GACR, project number 15-13415Y) and Ministry of Culture of the Czech Republic (DKRVO 2017/15, National Museum, 00023272; to VG).

DATA ACCESSIBILITY

DNA sequences: GenBank accession numbers in Supporting Information (Table S1).

Sampling localities and voucher information for molecular data analyses and environmental niche models in Supporting Information (Table S1).

Geospatial bioclimatic layers for the current, middle Holocene, last glacial maximum and last interglacial: Dryad <https://doi.org/10.5061/dryad.vs76v>.

AUTHOR CONTRIBUTIONS

R.C.B. designed the project; R.C.B., G.B., M.B., D.C.B., M.B., A.C., J.M.D., E.G., V.G., C.K., J.K., S.L., P.J.M., Z.T.N., M.-O.R., D.M.P., B.L.S. and A.G.Z.-B. collected field samples; J.V. contributed historical climate data; R.C.B. and J.L.P. collected and analysed the data; all authors contributed funding to the project; R.C.B. wrote the manuscript with input from all authors.

REFERENCES

- Amiet, J.-L. (2012). *Les rainettes du Cameroun (Amphibiens Anoures)*. Nyons: Imprimerie Marque Déposée.
- Anthony, N. M., Johnson-Bawe, M., Jeffery, K., Clifford, S. L., Abernethy, K. A., Tutin, C. E., ... Bruford, M. W. (2007). The role of Pleistocene refugia and rivers in shaping gorilla genetic diversity in central Africa. *Proceedings of the National Academy of Sciences of the United States of America*, 104, 20432–20436.
- Avise, J. C. (2000). *Phylogeography: The history and formation of species*. Boston, MA: Harvard University Press.
- Barej, M. F., Rödel, M. O., Loader, S. P., Menegon, M., Gonwouo, L. N., Penner, J., ... Schmitz, A. (2014). Light shines through the spindrift—Phylogeny of African torrent frogs (Amphibia, Anura, Petropedetidae). *Molecular Phylogenetics and Evolution*, 71, 261–273.
- Bell, R. C. (2016). A new species of *Hyperolius* (Amphibia: Hyperoliidae) from Príncipe Island, Democratic Republic of São Tomé and Príncipe. *Herpetologica*, 72, 343–351.
- Bell, R. C., Drewes, R. C., Channing, A., Gvozdík, V., Kielgast, J., Lötters, S., ... Zamudio, K. R. (2015). Overseas dispersal of *Hyperolius* reed frogs from Central Africa to the oceanic islands of São Tomé and Príncipe. *Journal of Biogeography*, 42, 65–75.
- Bell, R. C., Drewes, R. C., & Zamudio, K. R. (2015). Reed frog diversification in the Gulf of Guinea: Overseas dispersal, the progression rule, and in situ speciation. *Evolution*, 69, 904–915.
- Bell, R. C., Mackenzie, J. B., Hickerson, M. J., Chavarria, K. L., Cunningham, M., Williams, S. E., & Mortiz, C. (2012). Comparative multi-locus phylogeography confirms multiple vicariance events in co-distributed rainforest frogs. *Proceedings of the Royal Society B: Biological Sciences*, 279, 991–999.
- Bellemain, E., & Ricklefs, R. E. (2008). Are islands the end of the colonization road? *Trends in Ecology and Evolution*, 23, 461–468.
- Bohoussou, K. H., Cornette, R., Akpatou, B., Colyn, M., Kerbis Peterhans, J. C., Kennis, J., ... Nicolas, V. (2015). The phylogeography of the rodent genus *Malacomys* suggests multiple Afrotropical Pleistocene lowland forest refugia. *Journal of Biogeography*, 42, 2049–2061.
- Bonier, F., Martin, P. R., & Wingfield, J. C. (2007). Urban birds have broader environmental tolerance. *Biology Letters*, 3, 670–673.
- Born, C., Alvarez, N., McKey, D., Ossari, S., Wickings, E. J., Hossaert-McKey, M., & Chevallier, M. H. (2011). Insights into the biogeographical history of the Lower Guinea Forest Domain: Evidence for the role of refugia in the intraspecific differentiation of *Aucoumea klaineana*. *Molecular Ecology*, 20, 131–142.
- Bouckaert, R., Heled, J., Kühnert, D., Vaughan, T., Wu, C.-H., Xie, D., ... Drummond, A. J. (2014). BEAST 2: A software platform for Bayesian evolutionary analysis. *PLoS Computational Biology*, 10, e1003537.
- Bowie, R. C. K., Fjeldså, J., Hackett, S. J., & Crowe, T. M. (2004). Molecular evolution in space and through time: mtDNA phylogeography of the Olive Sunbird (*Nectarinia olivacea/obscura*) throughout continental Africa. *Molecular Phylogenetics and Evolution*, 33, 56–74.
- Brown, J. L., Maan, M. E., Cummings, M. E., & Summers, K. (2010). Evidence for selection on coloration in a Panamanian poison frog: A coalescent-based approach. *Journal of Biogeography*, 37, 891–901.
- Bryant, D., & Moulton, V. (2004). Neighbor-Net: An agglomerative method for the construction of phylogenetic networks. *Molecular Biology and Evolution*, 21, 255–265.
- Bryja, J., Sumner, R., Kerbis Peterhans, J. C., Aghová, T., Bryjová, A., Mukula, O., ... Verheyen, E. (2017). Evolutionary history of the thicket rats (genus *Grammomys*) mirrors the evolution of African forests since late Miocene. *Journal of Biogeography*, 44, 182–194.
- Budde, K. B., González-Martínez, S. C., Hardy, O. J., & Heuertz, M. (2013). The ancient tropical rainforest tree *Symphonia globulifera* L. f. (Clusiaceae) was not restricted to postulated Pleistocene refugia in Atlantic Equatorial Africa. *Heredity*, 111, 66–76.
- Butynski, T. M., & Koster, S. H. (1994). Distribution and conservation status of primates in Bioko Island, Equatorial Guinea. *Biodiversity and Conservation*, 3, 893–909.
- Chown, S. L., Hoffmann, A. A., Kristensen, T. N., Angilletta, M. J., Jr, Stenseth, N. C., & Pertoldi, C. (2010). Adapting to climate change: A perspective from evolutionary physiology. *Climate Research*, 43, 3–15.
- Corl, A., Davis, A. R., Kuchta, S. R., & Sinervo, B. (2010). Selective loss of polymorphic mating types is associated with rapid phenotypic evolution during morphic speciation. *Proceedings of the National Academy of Sciences of the United States of America*, 107, 4254–4259.
- Couvreur, T. L., Chatrou, L. W., Sosef, M. S., & Richardson, J. E. (2008). Molecular phylogenetics reveal multiple tertiary vicariance origins of the African rain forest trees. *BMC Biology*, 6, 54.
- Damasceno, R., Strangas, M. L., Carnaval, A. C., Rodrigues, M. T., & Moritz, C. (2014). Revisiting the vanishing refuge model of diversification. *Frontiers in Genetics*, 5, 1–12.
- Dasmahapatra, K. K., Lamas, G., Simpson, F., & Mallet, J. (2010). The anatomy of a "suture zone" in Amazonian butterflies: A coalescent-based test for vicariant geographic divergence and speciation. *Molecular Ecology*, 19, 4283–4301.
- Dauby, G., Duminil, J., Heuertz, M., Koffi, G. K., Stévant, T., & Hardy, O. J. (2014). Congruent phylogeographical patterns of eight tree species

- in Atlantic Central Africa provide insights into the past dynamics of forest cover. *Molecular Ecology*, 23, 2299–2312.
- Dauby, G., Hardy, O. J., Leal, M., Breteler, F., & Stévant, T. (2014). Drivers of tree diversity in tropical rain forests: New insights from a comparison between littoral and hilly landscapes of Central Africa. *Journal of Biogeography*, 41, 574–586.
- Deruelle, B., Moreau, C., Nkoubou, C., Kambou, R., Lissom, J., Njofang, E., & Nono, A. (1991). The Cameroon Volcanic Line: A review. In A. B. Kampunzu, & R. T. Lubala (Eds.), *Magmatism in extensional structural settings* (pp. 274–327). Berlin: Springer.
- Droissart, V., Sonké, B., Hardy, O. J., Simo, M., Taedoumg, H., Nguembou, C. K., & Stévant, T. (2011). Do plant families with contrasting functional traits show similar patterns of endemism? A case study with Central African Orchidaceae and Rubiaceae. *Biodiversity and Conservation*, 20, 1507–1531.
- Drummond, A. J., Suchard, M. A., Xie, D., & Rambaut, A. (2012). Bayesian phylogenetics with BEAUti and the BEAST 1.7. *Molecular Biology and Evolution*, 29, 1969–1973.
- Duminil, J., Brown, R. P., Ewédjé E-E, B. K., Mardulyn, P., Doucet, J.-L., & Hardy, O. J. (2013). Large-scale pattern of genetic differentiation within African rainforest trees: Insights on the roles of ecological gradients and past climate changes on the evolution of *Erythrophloeum* spp. (Fabaceae). *BMC Evolutionary Biology*, 13, 195.
- Duminil, J., Mona, S., Mardulyn, P., Doumenge, C., Walmacq, F., Doucet, J.-L., & Hardy, O. J. (2015). Late Pleistocene molecular dating of past population fragmentation and demographic changes in African rain forest tree species supports the forest refuge hypothesis. *Journal of Biogeography*, 42, 1443–1454.
- Elith, J., Phillips, S. J., Hastie, T., Dudík, M., Chee, Y. E., & Yates, C. J. (2011). A statistical explanation of MaxEnt for ecologists. *Diversity and Distributions*, 17, 43–57.
- Evanno, G., Regnaut, S., & Goudet, J. (2005). Detecting the number of clusters of individuals using the software structure: A simulation study. *Molecular Ecology*, 14, 2611–2620.
- Evans, B. J., Carter, T. F., Greenbaum, E., Gvozdić, V., Kelley, D. B., McLaughlin, P. J., ... Blackburn, D. C. (2015). Genetics, morphology, advertisement calls, and historical records distinguish six new polyploid species of African clawed frog (*Xenopus*, Pipidae) from West and Central Africa. *PLoS One*, 10, e0142823.
- Excoffier, L., Laval, G., & Schneider, S. (2005). Arlequin (version 3.0): An integrated software package for population genetics data analysis. *Evolutionary Bioinformatics Online*, 1, 47.
- Faye, A., Deblauwe, V., Mariac, C., & Richard, D. (2016). Phylogeography of the genus *Podococcus* (Palmae/Arecaceae) in Central African rain forests: Climate stability predicts unique genetic diversity. *Molecular Phylogenetics and Evolution*, 105, 126–138.
- Fjeldsø, J., & Lovett, J. C. (1997). Geographical patterns of old and young species in African forest biota: The significance of specific montane areas as evolutionary centres. *Biodiversity and Conservation*, 6, 325–346.
- Fleming, K. M. (2000). *Glacial rebound and sea-level change: Constraints on the Greenland ice sheet*. Canberra: Australian National University.
- Fleming, K., Johnston, P., Zwart, D., et al. (1998). Refining the eustatic sea-level curve since the Last Glacial Maximum using far- and intermediate-field sites. *Earth and Planetary Science Letters*, 163, 327–342.
- Freedman, A. H., Thomassen, H. A., Buermann, W., & Smith, T. B. (2010). Genomic signals of diversification along ecological gradients in a tropical lizard. *Molecular Ecology*, 19, 3773–3788.
- Fuchs, J., Parra, J. L., Goodman, S. M., Raherilalao, M. J., VanDerWal, J., & Bowie, R. C. K. (2013). Extending ecological niche models to the past 120 000 years corroborates the lack of strong phylogeographic structure in the crested drongo (*Dicrurus forficatus*) on Madagascar. *Biological Journal of the Linnean Society*, 108, 658–676.
- Futuyama, D. J. (2010). Evolutionary constraint and ecological consequences. *Evolution*, 64, 1865–1884.
- Graham, C. H., VanDerWal, J., Phillips, S. J., Moritz, C., & Williams, S. E. (2010). Dynamic refugia and species persistence: Tracking spatial shifts in habitat through time. *Ecography*, 33, 1062–1069.
- Harcourt, A. H., & Wood, M. A. (2012). Rivers as barriers to primate distributions in Africa. *International Journal of Primatology*, 33, 168–183.
- Hardy, O. J., Born, C., Budde, K. B., Dainou, K., Dauby, G., Duminil, J., ... Koffi, G. K. (2013). Comparative phylogeography of African rain forest trees: A review of genetic signatures of vegetation history in the Guineo-Congolian region. *Comptes Rendus Geoscience*, 345, 284–296.
- Hasegawa, M., Kishino, H., & Yano, T. (1985). Dating of the human-ape splitting by a molecular clock of mitochondrial DNA. *Journal of Molecular Evolution*, 22, 160–174.
- Hassanin, A., Khoudier, S., Gembu, G.-C., Goodman, S. M., Kadjo, B., Nesi, N., ... Bonillo, C. (2015). The comparative phylogeography of fruit bats of the tribe Scotonycterini (Chiroptera, Pteropodidae) reveals cryptic species diversity related to African Pleistocene forest refugia. *Comptes Rendus Biologies*, 338, 197–211.
- Heled, J., & Drummond, A. J. (2008). Bayesian inference of population size history from multiple loci. *BMC Evolutionary Biology*, 8, 289.
- Heled, J., & Drummond, A. J. (2010). Bayesian inference of species trees from multilocus data. *Molecular Biology and Evolution*, 27, 570–580.
- Herman, J. S., & Searle, J. B. (2011). Post-glacial partitioning of mitochondrial genetic variation in the field vole. *Proceedings of the Royal Society B: Biological Sciences*, 278, 3601–3607.
- Heuertz, M., Duminil, J., Dauby, G., Savolainen, V., & Hardy, O. J. (2014). Comparative phylogeography in rainforest trees from Lower Guinea, Africa. *PLoS One*, 9, e84307.
- Hickerson, M. J., Stahl, E. A., & Lessios, H. A. (2006). Test for simultaneous divergence using approximate Bayesian computation. *Evolution*, 60, 2435–2453.
- Hijmans, R. J., Cameron, S. E., Parra, J. L., Jones, P. G., & Jarvis, A. (2005). Very high resolution interpolated climate surfaces for global land areas. *International Journal of Climatology*, 25, 1965–1978.
- Holstein, N., & Renner, S. S. (2011). A dated phylogeny and collection records reveal repeated biome shifts in the African genus *Coccinia* (Cucurbitaceae). *BMC Evolutionary Biology*, 11, 28.
- Hugall, A. F., Moritz, C., Moussalli, A., & Stanislav, J. (2002). Reconciling paleodistribution models and comparative phylogeography in the Wet Tropics rainforest land snail *Gnarosophia bellendenkerensis* (Brazier 1875). *Proceedings of the National Academy of Sciences of the United States of America*, 99, 6112–6117.
- Hugall, A. F., & Stuart-Fox, D. M. (2012). Accelerated speciation in colour-polymorphic birds. *Nature*, 485, 631–634.
- Huntley, J. W., & Voelker, G. (2016). Cryptic diversity in Afro-tropical lowland forests: The systematics and biogeography of the avian genus *Bleda*. *Molecular Phylogenetics and Evolution*, 99, 297–308.
- Huson, D. H., & Bryant, D. (2006). Application of phylogenetic networks in evolutionary studies. *Molecular Biology and Evolution*, 23, 254–267.
- Jacquet, F., Denys, C., Verheyen, E., Bryja, J., Hutterer, R., Kerbis Peterhand, J. C., ... Nicolas, V. (2015). Phylogeography and evolutionary history of the *Crocodylus olivieri* complex (Mammalia, Soricomorpha): From a forest origin to broad ecological expansion across Africa. *BMC Evolutionary Biology*, 15, 71.
- Jenkins, C. N., Pimm, S. L., & Joppa, L. N. (2013). Global patterns of terrestrial vertebrate diversity and conservation. *Proceedings of the National Academy of Sciences of the United States of America*, 110, E2602–E2610.
- Johnston, A. R., & Anthony, N. M. (2012). A multi-locus species phylogeny of African forest duikers in the subfamily Cephalophinae: Evidence for a recent radiation in the Pleistocene. *BMC Evolutionary Biology*, 12, 120.
- Joly, S., & Bruneau, A. (2006). Incorporating allelic variation for reconstructing the evolutionary history of organisms from multiple genes:

- An example from *Rosa* in North America. *Systematic Biology*, 55, 623–636.
- Jones, P. J. (1994). Biodiversity in the Gulf of Guinea: An overview. *Biodiversity and Conservation*, 3, 772–784.
- Kadu, C. A. C., Schueler, S., Konrad, H., Muluvi, G. M. M., Eyog-Matig, O., Muchugi, A., ... Geburek, T. (2011). Phylogeography of the Afromontane *Prunus africana* reveals a former migration corridor between East and West African highlands. *Molecular Ecology*, 20, 165–178.
- Kindler, C., Moosig, M., Branch, W. R., Harvey, J., Kehlmaier, C., Nagy, Z. T., ... Fritz, U. (2016). Comparative phylogeographies of six species of hinged terrapins (*Pelusios* spp.) reveal discordant patterns and unexpected differentiation in the *P. castaneus*/*P. chapini* complex and *P. rhodesianus*. *Biological Journal of the Linnean Society*, 117, 305–321.
- Kirschel, A. N. G., Slabbekoorn, H., Blumstein, D. T., Cohen, R. E., de Kort, S. R., Buermann, W., & Smith, T. B. (2011). Testing alternative hypotheses for evolutionary diversification in an African songbird: Rainforest refugia versus ecological gradients. *Evolution*, 65, 3162–3174.
- Koffi, G. K., Hardy, O. J., Doumenge, C., Cruaud, C., & Heuertz, M. (2011). Diversity gradients and phylogeographic patterns in *Santiria trimera* (Burseraceae), a widespread African tree typical of mature rainforests. *American Journal of Botany*, 98, 254–264.
- Lanfear, R., Calcott, B., Ho, S. Y. W., & Guindon, S. (2012). PartitionFinder: Combined selection of partitioning schemes and substitution models for phylogenetic analyses. *Molecular Biology and Evolution*, 29, 1695–1701.
- Larkin, M. A., Blackshields, G., Brown, N. P., Chenna, R., McGettigan, P. A., McWilliam, H., ... Higgins, D. G. (2007). Clustal W and Clustal X version 2.0. *Bioinformatics*, 23, 2947–2948.
- Laurent, R. F. (1943). Les *Hyperolius* (Batraciens) du Musée du Congo. *Annales du Musée Royal du Congo Belge. Sciences Zoologiques. Tervuren*, 4, 61–140.
- Laurent, R. F. (1956). Notes herpétologiques africaines I. *Revue de Zoologie et de Botanique Africaines*, 52, 229–256.
- Laurent, R. F. (1976). Nouveaux commentaires sur la superespèce *Hyperolius viridiflavus* (Anura). Musée Royal d'Afrique Centrale Série IN-8. *Science Zoologique*.
- Lea, D. W., Martin, P. A., Pak, D. K., & Spero, H. J. (2002). Reconstructing a 350 ky history of sea level using planktonic Mg/Ca and oxygen isotope records from a Cocos Ridge core. *Quaternary Science Reviews*, 21, 283–293.
- Leaché, A. D., Crews, S. C., & Hickerson, M. J. (2007). Two waves of diversification in mammals and reptiles of Baja California revealed by hierarchical Bayesian analysis. *Biology Letters*, 3, 646–650.
- Leaché, A. D., & Fujita, M. K. (2010). Bayesian species delimitation in West African forest geckos (*Hemidactylus fasciatus*). *Proceedings of the Royal Society B: Biological Sciences*, 277, 3071–3077.
- Leache, A. D., Fujita, M. K., Minin, V. N., & Bouckaert, R. R. (2014). Species delimitation using genome-wide SNP data. *Systematic Biology*, 63, 534–542.
- Lewin, A., Feldman, A., Bauer, A. M., Belmaker, J., Broadley, D. G., Chirio, L., ... Meiri, S. (2016). Patterns of species richness, endemism and environmental gradients of African reptiles. *Journal of Biogeography*, 43, 2380–2390.
- Ley, A. C., Dauby, G., Koehler, J., Wypior, C., Roeser, M., & Hardy, O. J. (2014). Comparative phylogeography of eight herbs and lianas (Marantaceae) in central African rainforests. *Frontiers in Genetics*, 5, 403.
- Librado, P., & Rozas, J. (2009). DnaSP v5: A software for comprehensive analysis of DNA polymorphism data. *Bioinformatics*, 25, 1451–1452.
- Linder, H. P., de Klerk, H. M., Born, J., Burgess, N. D., Fjeldså, J., & Rahbek, C. (2012). The partitioning of Africa: Statistically defined biogeographical regions in sub-Saharan Africa. *Journal of Biogeography*, 39, 1189–1205.
- Lobo, J. M., Jiménez-Valverde, A., & Real, R. (2008). AUC: A misleading measure of the performance of predictive distribution models. *Global Ecology and Biogeography*, 17, 145–151.
- López-Urbe, M. M., Zamudio, K. R., Cardoso, C. F., & Danforth, B. N. (2014). Climate, physiological tolerance and sex-biased dispersal shape genetic structure of Neotropical orchid bees. *Molecular Ecology*, 23, 1874–1890.
- Lötters, S., & Schmitz, A. (2004). A new species of tree frog (Amphibia; *Hyperolius*) from the Bakossi Mountains, South-West-Cameroon. *Bonner zoologische Beiträge*, 52, 149–154.
- Lowe, A. J., Harris, D., Dormontt, E., & Dawson, I. K. (2010). Testing putative African tropical forest refugia using chloroplast and nuclear DNA phylogeography. *Tropical Plant Biology*, 3, 50–58.
- Maley, J. (1996). The African rain forest—Main characteristics of changes in vegetation and climate from the Upper Cretaceous to the Quaternary. *Proceedings of the Royal Society of Edinburgh. Section B. Biological Sciences*, 104, 31–73.
- Marzoli, A., Piccirillo, E. M., Renne, P. R., Bellieni, G., Iacumin, M., Nyobe, J. B., & Tongwa, A. T. (2000). The Cameroon volcanic line revisited: Petrogenesis of continental basaltic magmas from lithospheric and asthenospheric mantle sources. *Journal of Petrology*, 41, 87–109.
- Massatti, R., & Knowles, L. L. (2014). Microhabitat differences impact phylogeographic concordance of codistributed species: Genomic evidence in montane sedges (*Carex* L.) from the rocky mountains. *Evolution*, 68, 2833–2846.
- McRae, B. H. (2006). Isolation by resistance. *Evolution*, 60, 1551–1561.
- McRae, B. H., & Beier, P. (2007). Circuit theory predicts gene flow in plant and animal populations. *Proceedings of the National Academy of Sciences of the United States of America*, 104, 19885–19890.
- McRae, B. H., Dickson, B. G., Keitt, T. H., & Shah, V. B. (2008). Using circuit theory to model connectivity in ecology, evolution, and conservation. *Ecology*, 89, 2712–2724.
- Melo, M., Warren, B. H., & Jones, P. J. (2011). Rapid parallel evolution of aberrant traits in the diversification of the Gulf of Guinea white-eyes (Aves, Zosteropidae). *Molecular Ecology*, 20, 4953–4967.
- Meyers, J. B., Rosendahl, B. R., Harrison, C. G., & Ding, Z.-D. (1998). Deep-imaging seismic and gravity results from the offshore Cameroon Volcanic Line, and speculation of African hotlines. *Tectonophysics*, 284, 31–63.
- Milne, I., Lindner, D., Bayer, M., Husmeier, D., McGuire, G., Marshall, D. F., & Wright, F. (2009). TOPALi v2: A rich graphical interface for evolutionary analyses of multiple alignments on HPC clusters and multi-core desktops. *Bioinformatics*, 25, 126–127.
- Milne, G. A., Long, A. J., & Bassett, S. E. (2005). Modelling Holocene relative sea-level observations from the Caribbean and South America. *Quaternary Science Reviews*, 24, 1183–1202.
- Mitchell, M. W., Locatelli, S., Sesink Clee, P. R., Thomassen, H. A., & Gonder, M. K. (2015). Environmental variation and rivers govern the structure of chimpanzee genetic diversity in a biodiversity hotspot. *BMC Evolutionary Biology*, 15, 1.
- Muscarella, R., Galante, P. J., Soley-Guardia, M., Boria, R. A., Kass, J. M., Uriarte, M., & Anderson, R. P. (2014). ENMeval: An R package for conducting spatially independent evaluations and estimating optimal model complexity for Maxent ecological niche models. *Methods in Ecology and Evolution*, 5, 1198–1205.
- Nicolas, V., Missou, A. D., Denys, C., Kerbis Peterhans, J. C., Katuala, P., Couloux, A., & Colyn, M. (2011). The roles of rivers and Pleistocene refugia in shaping genetic diversity in *Praomys misonnei* in tropical Africa. *Journal of Biogeography*, 38, 191–207.
- Njabo, K. Y., Bowie, R. C. K., & Sorenson, M. D. (2008). Phylogeny, biogeography and taxonomy of the African wattle-eyes (Aves: Passeriformes: Platysteiridae). *Molecular Phylogenetics and Evolution*, 48, 136–149.

- Olson, D. M., & Dinerstein, E. (2001). Terrestrial ecoregions of the world: A new map of life on earth. *BioScience*, 51, 933–938.
- Pabijan, M., Wollenberg, K. C., & Vences, M. (2012). Small body size increases the regional differentiation of populations of tropical mantellid frogs (Anura: Mantellidae). *Journal of Evolutionary Biology*, 25, 2310–2324.
- Papadopoulou, A., & Knowles, L. L. L. (2015). Species-specific responses to island connectivity cycles: Refined models for testing phylogeographic concordance across a Mediterranean Pleistocene Aggregate Island Complex. *Molecular Ecology*, 24, 4252–4268.
- Papadopoulou, A., & Knowles, L. L. L. (2016). Toward a paradigm shift in comparative phylogeography driven by trait-based hypotheses. *Proceedings of the National Academy of Sciences of the United States of America*, 113, 8018–8024.
- Paz, A., Ibáñez, R., Lips, K. R., & Crawford, A. J. (2015). Testing the role of ecology and life history in structuring genetic variation across a landscape: A trait-based phylogeographic approach. *Molecular Ecology*, 24, 3723–3737.
- Pérez, J. D. V., Fa, J. E., Castroviejo, J., & Purroy, F. J. (1994). Species richness and endemism of birds in Bioko. *Biodiversity and Conservation*, 3, 868–892.
- Perret, J. L. (1975). Les sous-espèces d'*Hyperolius ocellatus* Günther (Amphibia, Salientia). *Annales de la Faculté des Sciences du Cameroun. Yaoundé*, 20, 23–31.
- Peterson, A. T., Papeş, M., & Soberón, J. (2008). Rethinking receiver operating characteristic analysis applications in ecological niche modeling. *Ecological Modelling*, 213, 63–72.
- Phillips, S. J., Anderson, R. P., & Schapire, R. E. (2006). Maximum entropy modeling of species geographic distributions. *Ecological Modelling*, 190, 231–259.
- Plana, V. (2004). Mechanisms and tempo of evolution in the African Guineo-Congolian rainforest. *Philosophical Transactions of the Royal Society B: Biological Sciences*, 359, 1585–1594.
- Portik, D. M. (2015). *Diversification of Afrobatrachian frogs and the herpetofauna of the Arabian Peninsula*. Berkeley: University of California.
- Portik, D. M., Jongsma, G. F. M., Kouete, M. T., Scheinberg, L. A., Freiermuth, B., Tapondjou, W. P., & Blackburn, D. C. (2016). A survey of amphibians and reptiles in the foothills of Mount Kupe, Cameroon. *Amphibian and Reptile Conservation*, 10, 37–67.
- Pritchard, J. K., Stephens, M., & Donnelly, P. (2000). Inference of population structure using multilocus genotype data. *Genetics*, 155, 945–959.
- Quéroil, S., Verheyen, E., Dillen, M., & Colyn, M. (2003). Patterns of diversification in two African forest shrews: *Sylvisorex johnstoni* and *Sylvisorex ollula* (Soricidae, Insectivora) in relation to paleo-environmental changes. *Molecular Phylogenetics and Evolution*, 28, 24–37.
- Rambaut, A., Suchard, M. A., Xie, D., & Drummond, A. J. (2013). *Tracer*. Retrieved from <http://beast.bio.ed.ac.uk/Tracer>.
- Rodríguez, A., Börner, M., Pabijan, M., Gehara, M., Haddad, C. F. B., & Vences, M. (2015). Genetic divergence in tropical anurans: Deeper phylogeographic structure in forest specialists and in topographically complex regions. *Evolutionary Ecology*, 29, 765–785.
- Salthe, S. N., & Duellman, W. E. (1973). Quantitative constraints associated with reproductive mode in anurans. In J. L. Vial (Ed.), *Evolutionary biology of the anurans* (pp. 229–249). Kansas City: University of Missouri Press.
- Sanguila, M. B., Siler, C. D., Diesmos, A. C., Nuñez, O., & Brown, R. M. (2011). Phylogeography, geographic structure, genetic variation, and potential species boundaries in Philippine slender toads. *Molecular Phylogenetics and Evolution*, 61, 333–350.
- Schick, S., Kielgast, J., Rödder, D., Muchai, V., Burger, M., & Lötters, S. (2010). New species of reed frog from the Congo basin with discussion of paraphyly in Cinnamon-belly reed frogs. *Zootaxa*, 2501, 23–36.
- Schiøtz, A. (1999). *Treefrogs of Africa*. Frankfurt am Main: Edition Chimaira.
- Shine, R. (1979). Sexual selection and sexual dimorphism in the Amphibia. *Copeia*, 1979, 297–306.
- Sinervo, B., & Lively, C. M. (1996). The rock-paper-scissors game and the evolution of alternative male strategies. *Nature*, 30, 240–243.
- Singarayer, J. S., & Valdes, P. J. (2010). High-latitude climate sensitivity to ice-sheet forcing over the last 120 kyr. *Quaternary Science Reviews*, 29, 43–55.
- Singhal, S., & Moritz, C. (2013). Reproductive isolation between phylogeographic lineages scales with divergence. *Proceedings of the Royal Society B: Biological Sciences*, 280, 20132246.
- Smith, T. B., Calsbeek, R., Wayne, R. K., Holder, K. H., Pires, D., & Bardeleben, C. (2005). Testing alternative mechanisms of evolutionary divergence in an African rain forest passerine bird. *Journal of Evolutionary Biology*, 18, 257–268.
- Smith, T. B., Thomassen, H. A., Freedman, A. H., Sehgal, R. N. M., Buermann, W., Saatchi, S., ... Wayne, R. K. (2011). Patterns of divergence in the olive sunbird *Cyanomitra olivacea* (Aves: Nectariniidae) across the African rainforest–savanna ecotone. *Biological Journal of the Linnean Society*, 103, 821–835.
- Smith, T. B., Wayne, R. K., Girman, D. J., & Bruford, M. W. (1997). A role for ecotones in generating rainforest biodiversity. *Science*, 276, 1855–1857.
- Soberón, J. (2007). Grinnellian and Eltonian niches and geographic distributions of species. *Ecology Letters*, 10, 1115–1123.
- Stephens, M., Smith, N. J., & Donnelly, P. (2001). A new statistical method for haplotype reconstruction from population data. *American Journal of Human Genetics*, 68, 978–989.
- Swofford, D. L. (2003). *PAUP*: Phylogenetic analysis using parsimony (* and other methods)* Software program, Version: 4.0. Sunderland MA: Sinauer Associates.
- Telfer, P. T., Souquiere, S., Clifford, S. L., Abernethy, K. A., Bruford, M. W., Disotell, T. R., ... Wickings, E. J. (2003). Molecular evidence for deep phylogenetic divergence in *Mandrillus sphinx*. *Molecular Ecology*, 12, 2019–2024.
- Tosi, A. J. (2008). Forest monkeys and Pleistocene refugia: A phylogeographic window onto the disjunct distribution of the *Chlorocebus lhoesti* species group. *Zoological Journal of the Linnean Society*, 154, 408–418.
- VanDerWal, J., Beaumont, L., Zimmermann, N. E., & Lorch, P. (2011). *Climates: Methods for working with weather and climate*. Retrieved from www.rforge.net.
- Vanzolini, P. E., & Williams, E. E. (1981). The vanishing refuge: A mechanism for ecogeographic speciation. *Papéis Avulsos de Zoologia*, 34, 251–255.
- Voelker, G., Marks, B. D., Kahindo, C., A'genonga, U., Bapeamoni, F., Duffie, L. E., ... Light, J. E. (2013). River barriers and cryptic biodiversity in an evolutionary museum. *Ecology and Evolution*, 3, 536–545.
- Weber, L. C., VanDerWal, J., Schmidt, S., McDonald, W. J. F., & Shoo, L. P. (2014). Patterns of rain forest plant endemism in subtropical Australia relate to stable mesic refugia and species dispersal limitations. *Journal of Biogeography*, 41, 222–238.
- Weir, J. T., & Price, T. D. (2011). Limits to speciation inferred from times to secondary sympatry and ages of hybridizing species along a latitudinal gradient. *American Naturalist*, 177, 462–469.
- Wiens, J. J., Ackerly, D. D., Allen, A. P., Anacker, B. L., Buckley, L. B., Cornell, H. V., ... Stephens, P. R. (2010). Niche conservatism as an emerging principle in ecology and conservation biology. *Ecology Letters*, 13, 1310–1324.
- Winger, B. M., & Bates, J. M. (2015). The tempo of trait divergence in geographic isolation: Avian speciation across the Marañón Valley of Peru. *Evolution*, 69, 772–787.

- Wollenberg, K. C., Vieites, D. R., Glaw, F., & Vences, M. (2011). Speciation in little: The role of range and body size in the diversification of Malagasy mantellid frogs. *BMC Evolutionary Biology*, 11, 217.
- Zamudio, K. R., Bell, R. C., & Mason, N. A. (2016). Phenotypes in phylogeography: Species' traits, environmental variation, and vertebrate diversification. *Proceedings of the National Academy of Sciences of the United States of America*, 113, 8041–8048.
- Zimkus, B. M., & Gvoždík, V. (2013). Sky Islands of the Cameroon Volcanic Line: A diversification hot spot for puddle frogs (Phrynobatrachidae: *Phrynobatrachus*). *Zoologica Scripta*, 42, 591–611.
- Zimkus, B. M., Lawson, L. P., Barej, M. F., Barratt, C. D., Channing, A., Dash, K. M., ... Lötters, S. (2017). Leapfrogging into new territory: How Mascarene ridged frogs diversified across Africa and Madagascar to maintain their ecological niche. *Molecular Phylogenetics and Evolution*, 106, 254–269.

SUPPORTING INFORMATION

Additional Supporting Information may be found online in the supporting information tab for this article.

How to cite this article: Bell RC, Parra JL, Badjedjea G, et al. Idiosyncratic responses to climate-driven forest fragmentation and marine incursions in reed frogs from Central Africa and the Gulf of Guinea Islands. *Mol Ecol*. 2017;26:5223–5244. <https://doi.org/10.1111/mec.14260>